Symmetry-adapted cluster and symmetry-adapted cluster-configuration interaction method in the polarizable continuum model: Theory of the solvent effect on the electronic excitation of molecules in solution

Roberto Cammi,[1,a)] Ryoichi Fukuda,[2,3,b)] Masahiro Ehara,[2,3,c)] and Hiroshi Nakatsuji[3,4,d)]
[1]*Dipartmento di Chimica, Università di Parma, Viale delle Scienze 17/A, 43100 Parma, Italy*
[2]*Department of Theoretical and Computational Molecular Science, Institute for Molecular Science and Research Center for Computational Science, 38 Nishigo-Naka, Myodaiji, Okazaki 444-8585, Japan*
[3]*Japan Science and Technology Agency, CREST, Sanboncho-5, Chiyoda-ku, Tokyo 102-0075, Japan*
[4]*Quantum Chemistry Research Institute, Kyodai Katsura Venture Plaza, 1-36 Goryo Oohara, Nishikyo-ku, Kyoto 615-8245, Japan*

(Received 30 March 2010; accepted 2 June 2010; published online 13 July 2010)

In this paper we present the theory and implementation of the symmetry-adapted cluster (SAC) and symmetry-adapted cluster-configuration interaction (SAC-CI) method, including the solvent effect, using the polarizable continuum model (PCM). The PCM and SAC/SAC-CI were consistently combined in terms of the energy functional formalism. The excitation energies were calculated by means of the state-specific approach, the advantage of which over the linear-response approach has been shown. The single-point energy calculation and its analytical energy derivatives are presented and implemented, where the free-energy and its derivatives are evaluated because of the presence of solute-solvent interactions. We have applied this method to s-*trans*-acrolein and metylenecyclopropene of their electronic excitation in solution. The molecular geometries in the ground and excited states were optimized in vacuum and in solution, and both the vertical and adiabatic excitations were studied. The PCM-SAC/SAC-CI reproduced the known trend of the solvent effect on the vertical excitation energies but the shift values were underestimated. The excited state geometry in planar and nonplanar conformations was investigated. The importance of using state-specific methods was shown for the solvent effect on the optimized geometry in the excited state. The mechanism of the solvent effect is discussed in terms of the Mulliken charges and electronic dipole moment. © *2010 American Institute of Physics*. [doi:10.1063/1.3456540]

I. INTRODUCTION

Electronic excitations of molecules and molecular systems in particular circumstances, such as in solutions, have attracted attention for a long time. Solvatochromism, the shift of transition energies by a solvent, is an important consideration in such research.[1] Photochemical and electrochemical reactions in solution are other considerations.[2] Several states with different electron density distributions may exist in a small energy width, and therefore their relative energy levels can be strongly influenced by solute-solvent interactions. The latter can change the features of a potential energy surface and the transition probability between electronic states. Solvents affect the efficiency of chemical processes—a reaction path or mechanism can be alternated by a solvent. Many photochemical and electrochemical processes involve several electronic states, not only the initial and final states but also intermediate states. Reliable computational studies are essential for elucidating the mechanism of such complex processes because it is difficult to detect short-lived intermediate states in certain solvents experimentally. There is a strong demand for the development of theoretical and computational methods to understand photochemical and electrochemical phenomena in solution, such as those associated with utilizing photoenergy with functional dyes, organic photovoltaic cells, charge transport in batteries and molecular devices, etc.[3] This study reports theoretical and computational methods in the framework of the symmetry-adapted cluster (SAC) and symmetry-adapted cluster-configuration interaction (SAC-CI) method, in terms of the polarizable continuum model (PCM).

The SAC/SAC-CI method is a theory for the ground and excited states of molecules based on the coupled-cluster (CC) theory that was proposed by Nakatsuji and co-workers[4,5] in 1977, and has since then been extensively developed. Other CC based theories, such as the equation-of-motion (EOM),[6] linear-response (LR) and time-dependent[7,8] CC theories are closely related to the SAC/SAC-CI theory. The SAC/SAC-CI theory describes the totally symmetric singlet state (usually the ground state) with the SAC expansion. The excitations from the SAC state are expressed by the CI-like eigenvalue problem. The electron correlation in excited states is considered on the basis of the correlated ground state wave function; therefore, the wave functions of excited states are expressed in a compact and well-balanced form. Furthermore, the obtained states are orthogonal to each other, which is a necessary condition for excited states. For recent reviews of the SAC/SAC-CI method, see Ref. 9.

[a)]Electronic mail: chifi@unipr.it.
[b)]Electronic mail: fukuda@ims.ac.jp.
[c)]Electronic mail: ehara@ims.ac.jp.
[d)]Electronic mail: h.nakatsuji@qcri.or.jp.

The PCM method introduces solvent effects in the quantum mechanical (QM) description of the solute by using a representation of the solvent as a continuum responsive distribution. The PCM model was proposed by Tomasi and co-workers[10] in 1981 and since then has been continuously developed. For a recent review of the PCM method see Ref. 11. The procedure is based on the definition of an effective Hamiltonian, formally composed of the solute Hamiltonian accompanied by solute-solvent integral interaction operators. The solution of the effective Schrödinger equation is obtained with an iterative procedure because the solute-solvent interaction operator depends on the QM charge distribution of the solute. The solute-solvent interaction may include the electrostatic component of the solute-solvent interaction and the nonelectrostatic component.

In the present study, the PCM method has been combined with the SAC/SAC-CI method with an energy functional approach, which provides a general and consistent formulation for the PCM method with nonvariational wave functions. Furthermore, the extension to the analytical energy gradient method is straightforward with the energy functional formalism. The energy functional method was originally introduced into the CC theory by Arponen and co-workers,[12] and further systematically developed by Bartlett and co-workers[13] and by a Scandinavian school.[14,15] The method offers an alternative, variational-like derivation of the CC equations and is compatible with the generalized Hellman–Feynman theorem for the calculation of the response properties.

Originally two versions of the SAC method were proposed:[4,5] a SAC-nonvariational (SAC-NV) and an approximate SAC-variational (SAC-V). When applying the variational principle to an expression of the SAC expectation value of the electronic energy, we can obtain the variational SAC formalism. This variational solution is very difficult to determine and some approximations have to be introduced because of the nonclosed form of the SAC expectation value of the energy. Thus, we will not address the SAC-V method here. In the SAC-NV method, the SAC wave function (ket vector) satisfies the Schrödinger equation that is projected into the left side of the subspace of the reference [Hartree–Fock (HF)] state and the corresponding linked excited configurations.

The SAC energy functional approach is based on an expectation value of the energy, as the SAC variational but with a variation in the latter: the left (bra) SAC vector is not a Hermitian conjugate of the right (ket) SAC vector, and it is parametrized in a different way. This form of the energy expectation value is called a SAC energy functional. A stationary principle leads to the equations for the SAC right vector and for the SAC left vector. The right equation corresponds to the SAC-NV equations. The left equation allows the study of molecular response properties, including analytical gradients. This energy functional formulation has resulted in the SAC and Z-vector of SAC (Z-SAC) equations that are already known.[16] However, energy functional formulation is necessary for the development of PCM in the CC theory.[17] We note that an energy functional (Lagrangian) formulation was first proposed in solvent theory by Christiansen *et al.*[15] The SAC energy functional is further addressed in the following section.

A clear description of the interplay between the electronic correlation and solvation is key to the application of the PCM solvation method to the QM correlated method. The introduction of the correlation modifies the total charge distribution and, consequently, the solvent polarization charges are also changed. In turn, the polarization charges modify the electron correlation effect. The decoupling of these effects was elaborated on, in 1991, by Olivares del Valle and the Pisa group, using the many-body perturbation theory,[18] and extended by one of the present authors to the CC theory.[17] In brief, the method introduces two computational levels: (1) the noniterative scheme (originally called PTE[18]) in which the solvated HF orbitals are used to compute the correlation energy and (2) an iterative scheme (originally called PTED[18]) in which the reaction field is partitioned into a HF contribution and a pure correlative contribution, and the solvated correlated density usually has a self-consistent reaction field. The latter approach will be extended here to the SAC theory. The former PTE approach is rather simple and has already been applied to SAC-CI calculations in vertical excitations in solution,[19] in which the solvated HF offers a good approximation of the solvent effect. For a more sophisticated theory, however, the PTED approach with nonequilibrium solvation is required, even for vertical excitations in solution.

The analytical expression of the energy derivatives is essential for computational methods addressing chemical problems. We will consider the analytical formulation of the first derivatives of the SAC and SAC-CI energies with respect to nuclear coordinates, although there is a large variety of derivatives appearing in molecular calculations.[16,20] The iterative PTED approach is necessary for the geometry optimization of the excited state in solution with the SAC-CI because the HF solvation is no longer a good approximation of the solvation for the target state of optimization.

Two approaches are generally used to obtain the electronic excitation energies with QM continuum solvation models. The first one, denoted as the state-specific (SS) approach, is based on the CI-like explicit description of the electronic wave functions of excited states. The second one is based on the LR theory.[21] The SS method is based on the definition of an effective Hamiltonian, in which the solute-solvent interaction operator depends on the QM charge distribution of the solute in the specific excited state. In the SS method, the solution of the effective Schrödinger equation is obtained using an iterative procedure. Different states are individually solved within their specific solvations. Here, it should be noted that the obtained states are not rigorously orthogonal to each other. In this article we use the term "SS" as "SS solvation," not for "SS excited states theory" such as multiconfigurational self-consistent field (MCSCF) calculations.

The second approach is based on a Hamiltonian with explicit time dependence, provided with an appropriate form of the time-dependent variation principle (the Frenkel principle[22] is generally used here). Using this as a starting

point, linear and nonlinear response functions are derived. The electronic excitation energies are obtained as poles of the LR functions. Today the LR functions are widely used both in gas phase and in solution for the characterization of excited states and molecular properties. Although the complete equivalence between SS and LR results for the excitation energies has been universally accepted, recently it was shown[23] that this equivalence is valid only in vacuum and that LR results can be seriously different in solution.[21,24–26] The PCM-SAC-CI that we will present in this study involves the SS approach.

Another aspect of the description of excited states in solution is the nonequilibrium solvation effects.[27] Electronic transitions are very fast and here the solvent molecules have no time to rearrange themselves, except for the electronic component of the solvent polarization, whose relaxation time is of the same order as that of vertical electronic transition. This effect means that the energy (free-energy in this case) of the vertical transition has a component due to the solvent interaction, which is limited to changes in the fast electronic polarization. The effects of the electronic transition continue with time but these are not regarded as a vertical process and have to be described with a different formulation of the continuum method.[27]

The formulation that we report here refers to the equilibrium formulation. For the nonequilibrium formulation there are two versions, the Marcus and Pekar partitions,[28,29] which describe this simple process. They differ in the intermediate stages of the elaboration of the problem but arrive at the same result when the correct expression for the nonequilibrium free-energy functional is used.[30] The formulation corresponding to the Pekar partition can be directly obtained from the equilibrium case by substituting the polarization charges of the solvent that appear in the PCM-SAC-CI equations derived in this study with those corresponding to the nonequilibrium case.[21,25]

There are several methods for the description of electronic excited states in solution. As solvent models, basically two approaches are available: a discrete representation and a continuous responsive distribution. A typical discrete model may be the quantum mechanics and molecular mechanics (QM/MM) approach,[30,31] while the PCM is a representative of a continuous model. For the description of an excited state, we have to consider the polarization of solvent charges caused by the electronic excitation. This polarization is suitably described within the PCM model using the nonequilibrium solvation approach, while it requires a polarizable force field for the QM/MM method.[32,33] This issue involves computationally expensive procedure[26] and most of the QM/MM approaches with electron correlation are still limited to the nonpolarizable force field. The rather simple PCM is suitable for electronic excitation. The polarizable continuum can offer a response to the electronic excitation. The characteristics of the electronic states of a solvent can be controlled by the dielectric constant ε parameter, as the nonequilibrium solvation is divided into fast and slow relaxations. This may be reasonable to describe the electronic excitation because its time-scale of response and relaxation is different from the coordination and orientation; usual classical models do not divide such effects.

Except for the configuration interaction with singles (CIS) method, the MCSCF and the time-dependent density functional theory (TDDFT) methods have been widely used for the calculation of electronic excited states in solution. The MCSCF is a variational method and it is a natural extension of the HF self-consistent field (SCF) in the ground state. In TDDFT, excited states are described by the LR theory, which is not always a good approach for solvent effects in excited states. To overcome this, an approximated SS approach for TDDFT has been proposed.[25] There are many reports on the vertical excitation that use the PTE approach with the PCM, QM/MM, and other solvent models. Such computational routes have become black-box methods in many recent program packages, and we will therefore not refer such studies here. For electronic excitation in solution, the SS and PTED approaches are required for general applications to various chemical and physical phenomena that include vertical and adiabatic transitions. The present study is the first implementation and application of the SS and PTED approach with electron correlation, but a related study on the EOM-CC has recently been reported.[34]

The primary objectives of the present work are as follows: (1) Formulate the SAC and SAC-CI theories and their analytical energy gradients in the PCM method using energy functional formulas; (2) implement the PCM-SAC and PCM-SAC-CI formulas in the latest version of the SAC-CI program;[35] (3) perform applications to s-*trans*-acrolein and methylencyclopropene, which are typical small molecules with characteristic solvation and excitation.

Acrolein is the smallest conjugating aldehyde, whose low-lying excited states have been widely studied. Their solvatochromism has been studied using various experimental[36–39] and theoretical[39–44] methods. The solvent effects on the lowest $n \rightarrow \pi$ and the lowest $\pi \rightarrow \pi^*$ excitation energies are opposite, and the mechanisms therefore have been proposed. Our results confirmed earlier findings about the vertical excitations. In our study we also performed the geometry optimization in the excited states, in vacuum, and in solution. A nonplanar geometry was found for the $\pi \rightarrow \pi^*$ state, which was not considered in our previous study.[45] The solvent effects on the excited state geometry and adiabatic excitations were studied in the present study. We examined the importance of relaxation in the electronic wave function and molecular geometry in the excited state. We have shown that the SS approach is essential to study the solvent effect on the excited state geometry.

Methylenecyclopropene is known for its "sudden polarization" due to electronic excitation.[46] The directions of its electronic dipole moment are opposite in the ground state and the lowest $\pi \rightarrow \pi^*$ state. Its significant solvent effect on the UV-visible spectrum has been reported,[47] and several theoretical studies have been carried out in efforts to clarify the mechanism of the solvatochromism.[48,49] Our results confirmed the earlier findings about the solvent effects on the vertical excitation. We also performed the geometry optimization of the excited states and found a local minimal struc-

ture of twisted conformation that we had not considered in a previous SAC-CI calculation.[16] The geometrical relaxation may significantly affect the position of the vertical transition in the UV-visible spectrum.

We introduced the SAC/SAC-CI theory of isolated molecules in a new formulation based on an energy functional approach, which is fundamentally the extension of the SAC/SAC-CI to the PCM method. The energy functional formalism of SAC/SAC-CI will be extended to the free-energy functional in solution by means of the PCM. We will present the theory in both state vector formalism and the Hamiltonian matrix representation for the purpose of comparison with previous papers on SAC-CI. The single-point energy and analytical energy gradient of the PCM-SAC/SAC-CI have been implemented in the latest SAC-CI program and combined with a GAUSSIAN program package.[50] In the practical algorithm in the program, we have used the latest molecular orbital (MO) integral-driven formalism because it is much more efficient.[35] Details of the MO integral formalism will be presented in a forthcoming paper.

II. THEORY

A. The SAC theory for isolated molecules in an energy functional approach

First we will summarize the SAC theory for isolated molecules in an energy functional approach because the approach enables the consistent formulation of the PCM-SAC. The SAC energy functional approach introduces distinct right and left SAC wave vectors, respectively, denoted by $|\Psi_{\mathrm{SAC}}\rangle$ and $\langle\Lambda'|$. The right SAC vector $|\Psi_{\mathrm{SAC}}\rangle$ is defined as the cluster expansion based on the reference function $|0\rangle$, which is usually the HF single determinant

$$|\Psi_{\mathrm{SAC}}\rangle = \exp(S)|0\rangle \quad \text{with} \quad S = \sum_I C_I S_I^\dagger, \tag{1}$$

where $S_I^\dagger$ is symmetry-adapted linked excitation operators, which discriminates between the SAC and the ordinary CC methods,[51] and C_I is the corresponding amplitudes. The left SAC vector $\langle\Lambda'|$ is written as the following configuration expansion form

$$\langle\Lambda'| = \langle 0|\sum_K Z_K^{\mathrm{SAC}} S_K, \tag{2}$$

where S_K is the de-excitation linked operators and Z_K is the corresponding amplitude. The SAC energy functional is defined in terms of the left and right SAC vectors as

$$L_{\mathrm{SAC}} = \langle\Lambda|H_N|\Psi_{\mathrm{SAC}}\rangle - \langle\Lambda'|\Psi_{\mathrm{SAC}}\rangle\langle 0|H_N|\Psi_{\mathrm{SAC}}\rangle. \tag{3}$$

Here we have introduced the auxiliary left vector $\langle\Lambda| = \langle 0| + \langle\Lambda'|$ and H_N is the Hamiltonian operator given by

$$H_N = H - E_{\mathrm{HF}}, \tag{4}$$

where H is the Hamiltonian of a given isolated molecule and $E_{\mathrm{HF}} = \langle 0|H|0\rangle$ is the HF energy of the reference state.

The stationary conditions of the SAC energy functional determine the equations for the SAC vectors. More specifically, the stationarity of L_{SAC} with respect to the $\{Z_K\}$ amplitudes gives the SAC equation for the parameters of the right SAC vector, while the stationarity with respect to the $\{C_K\}$ amplitudes gives the equation for the parameters of the left SAC vector. The SAC equation for the $\{C_K\}$ amplitudes may be written as

$$\langle 0|S_K(H_N - \Delta E_{\mathrm{SAC}})|\Psi_{\mathrm{SAC}}\rangle = 0, \tag{5}$$

where ΔE_{SAC} is the SAC correlation energy

$$\Delta E_{\mathrm{SAC}} = \langle 0|H_N|\Psi_{\mathrm{SAC}}\rangle. \tag{6}$$

The equation for the Z_K amplitudes of the left SAC vector may be written as

$$\langle\Lambda|H_N S_K^\dagger|\Psi_{\mathrm{SAC}}\rangle - \langle\Lambda'|S_K^\dagger|\Psi_{\mathrm{SAC}}\rangle\langle 0|H_N|\Psi_{\mathrm{SAC}}\rangle + \langle\Lambda'|\Psi_{\mathrm{SAC}}\rangle\langle 0|H_N S_K^\dagger|\Psi_{\mathrm{SAC}}\rangle = 0. \tag{7}$$

As expected, the SAC equations (5) and (6) correspond to the left-projection onto the reference and linked excited configurations of the Schrödinger equation for the SAC vector $|\Psi_{\mathrm{SAC}}\rangle$, while the SAC equation (7) is known as the Z-SAC equation.[16]

The SAC energy functional approach may also be formulated in a Hamiltonian matrix-driven form.[4,5] We will adopt the so-called SAC-A approximation in which linked terms include all the single (S_1) and selected double (S_2) excitations, and the unlinked terms include the quadruple-excitation operator as the product of the selected double-excitation operators S_2. Throughout this paper we represent the Hamiltonian matrix elements as

$$H_{IJ} = \langle 0|S_I H_N S_J^\dagger|0\rangle, \quad H_{I,JK} = \langle 0|S_I H_N S_J^\dagger S_K^\dagger|0\rangle \tag{8}$$

and the overlap matrices between the configurations as

$$S_{IJ} = \langle 0|S_I S_J^\dagger|0\rangle, \quad S_{I,JK} = \langle 0|S_I S_J^\dagger S_K^\dagger|0\rangle. \tag{9}$$

The SAC energy functional in the Hamiltonian matrix form may be written as

$$L_{\mathrm{SAC}} = \sum_I C_I \bar{H}_{0I}(1 - \tilde{S}) + \sum_K Z_K\left(H_{K0} + \sum_I C_I \bar{H}_{KI}\right), \tag{10}$$

where $\tilde{S}$ denotes the overlap between the left and right SAC vectors, $\tilde{S} = \Sigma_{KJ} Z_K C_J \bar{S}_{KJ}$, and the overbar denotes transformed matrix elements, such as

$$\bar{H}_{LI} = H_{LI} + \frac{1}{2}\sum_J C_J H_{L,IJ} \quad \text{and} \quad \bar{S}_{KI} = S_{KI} + \frac{1}{2}\sum_I C_J S_{K,IJ}. \tag{11}$$

Applying the stationary conditions to the left side of Eq. (10), we obtain the Hamiltonian matrix forms of the SAC equations as follows:

$$H_{K0} + \sum_I C_I(\bar{H}_{KI} - \Delta E_{\mathrm{SAC}}\bar{S}_{KI}) = 0, \tag{12}$$

$$\Delta E_{\mathrm{SAC}} = \sum_I C_I \bar{H}_{0I}, \tag{13}$$

and

$$\bar{\bar{H}}_{0L} + \sum_L Z_L^{\mathrm{SAC}} Y_{KL} = 0, \tag{14}$$

where the Hamiltonian matrix elements $\bar{\bar{H}}_{0L}$ and Y_{KI} are given by

$$\bar{\bar{H}}_{KI} = H_{KI} + \sum_J C_J H_{K,IJ} \tag{15}$$

and

$$Y_{KI} = \bar{\bar{H}}_{KI} - \Delta E_{\mathrm{SAC}} \bar{S}_{KI} - \left(\sum_J C_J \bar{S}_{KJ} \right) \bar{\bar{H}}_{0I}. \tag{16}$$

Equations (12)–(14) are the equation for the C amplitudes of the right SAC vector, the expression of the SAC correlation energy, and the equation for the Z amplitudes of the left SAC vector, respectively. The Hamiltonian matrix form shows explicitly that the first two SAC equations (12) and (13) do not contain any dependence on the Z amplitudes. They are therefore not coupled to the third SAC equation (14) and, as a result, their solution provides all the information needed to determine the right SAC vector $|\Psi_{\mathrm{SAC}}\rangle$ and the SAC correlation energy ΔE_{SAC}. However, solution of the Z-SAC equation (14) for the left SAC vector simplifies enormously the evaluation of the analytical gradients of the SAC correlation energy ΔE_{SAC}.[16]

When the stationary conditions are satisfied the SAC energy functional L_{SAC} reduces to the SAC energy, i.e., $L_{\mathrm{SAC}} = \Delta E_{\mathrm{SAC}}$. As a consequence, the determination of the analytical gradients of ΔE_{SAC} can be obtained in terms of the analytical gradients of L_{SAC}. The first derivative of the SAC energy functional $L_{\mathrm{SAC}}^a = \partial L_{\mathrm{SAC}} / \partial a$, with respect to a perturbation parameter a, may be written in the following Hamiltonian matrix form:

$$L_{\mathrm{SAC}}^a = \sum_I C_I \bar{H}_{0I}^a + \sum_K Z_K H_{K0}^a + \sum_{KI} Z_K C_I \bar{H}_{KI}^a - \sum_{KI} Z_K C_I \bar{S}_{KI} \sum_J C_J \bar{H}_{0J}^a, \tag{17}$$

where the superscript a on the Hamiltonian matrix elements denotes their derivatives with respect to the perturbation.

The analytical gradient equation (17) does not contain any derivative of the SAC amplitudes C_K as a consequence of the stationarity of the SAC energy functional with respect to the Z amplitudes. Equation (17) is equivalent to the expression of the analytical gradient of the SAC correlation energy given in Ref. 16.

The derivatives of the Hamiltonian matrix elements appearing in Eq. (17) may be expressed in terms of derivatives of the Fock matrix elements and of the two-electron repulsion integrals. The resulting expression of the SAC gradients involves the derivatives of the MO expansion coefficients with respect to the specific perturbation parameter a.[52] However, the computationally demanding evaluation of the derivatives of the MO coefficients may be avoided by using the interchange theorem approach.[53] The gradient equation (17) completes our presentation of the SAC theory for isolated molecules based on the energy functional approach. We have now introduced all that is required to formulate the SAC theory for solvated molecules, which will be presented in the following subsections.

B. The PCM-SAC: The reference wave function and the free-energy functional

The ground state PCM-SAC vectors are defined from Eqs. (1) and (2) using, as a reference state, the HF wave function of the solvated molecule,

$$|\Psi_{\mathrm{SAC}}\rangle = \exp(S)|\tilde{0}\rangle, \quad S = \sum_I C_I S_I^\dagger \tag{18}$$

and

$$\langle \Lambda' | = \langle \tilde{0} | \sum_K Z_K^{\mathrm{SAC}} S_K, \tag{19}$$

where $|\tilde{0}\rangle$ is obtained from the solution of the HF equations for the PCM model.[10] The PCM-HF equations differ from the ordinary HF operator in the gas phase for the presence of solvation terms in the HF operator. The solute-solvent interaction operators represent the interaction of an electron of the solute with the solvent polarization charges induced by the solute charge distribution. The PCM-HF equations correspond to an extremum of the PCM energy functional within the single determinant wave function approximation. The PCM energy functional has the thermodynamic status of a free-energy and it differs from the expectation value of the molecular Hamiltonian.

The PCM-SAC energy functional, which will be denoted as $L_{\mathrm{SAC}}^{\mathrm{PCM}}$, is a generalization of the PCM free-energy functional to molecular solutes as described by the SAC wave function.[11] In the PCM-SAC free-energy functional the solute-solvent interaction is expressed in terms of the classical Coulomb interaction between the QM charge distribution of the solute and a set of polarization charges that are partitioned into $\mathbf{Q}_{\mathrm{HF}}$ and $\Delta\mathbf{Q}_{\mathrm{SAC}}$: terms due to the HF one-electron density and the SAC (correlation) component of the one-electron density of the solute.

The PCM-SAC free-energy functional may be written as

$$L_{\mathrm{SAC}}^{\mathrm{PCM}} = \langle \Lambda | H_N^{\mathrm{HF}} | \Psi_{\mathrm{SAC}} \rangle - \langle \Lambda' | \Psi_{\mathrm{SAC}} \rangle \langle \tilde{0} | H_N^{\mathrm{HF}} | \Psi_{\mathrm{SAC}} \rangle + \tfrac{1}{2} \Delta Q_{\mathrm{SAC}} \cdot \Delta V_{\mathrm{SAC}}, \tag{20}$$

where H_N^{HF} is the Hamiltonian of the solute in the presence of the HF polarization charges, and ΔQ_{SAC} and ΔV_{SAC} are the SAC contributions to the polarization charge and to the electrostatic potential of the molecular solute, respectively. The first two terms of $L_{\mathrm{SAC}}^{\mathrm{PCM}}$ correspond to a SAC energy functional [see Eq. (3)] for the molecular solute in the presence of the fixed reaction field of the HF state, while the third term represents the SAC (electron correlation) component of the solute-solvent interaction. The Hamiltonian H_N^{HF} is given by

$$H_N^{\mathrm{HF}} = H_N + \mathbf{Q}_{\mathrm{HF}} V_N, \tag{21}$$

where H_N is the normal ordered Hamiltonian of the isolated molecule [see Eq. (4)], $\mathbf{Q}_{\mathrm{HF}}$ is a vector collecting the HF polarization charges, and V_N is a vector operator collecting the normal ordered electrostatic potential operators [see Eq.

(25) below] at the positions of the polarization charges. The HF polarization charges $\mathbf{Q}_{\mathrm{HF}}$ may be written as an expectation value of a polarization charge vector operator Q,[46,52]

$$\mathbf{Q}_{\mathrm{HF}} = \langle \tilde{0}|Q|\tilde{0}\rangle. \tag{22}$$

The SAC expectation value ΔQ_{SAC} and ΔV_{SAC} in the last term of $L_{\mathrm{SAC}}^{\mathrm{PCM}}$ in Eq. (20) may be written as

$$\Delta Q_{\mathrm{SAC}} = \langle \Lambda|Q_N|\Psi_{\mathrm{SAC}}\rangle - \langle \Lambda'|\Psi_{\mathrm{SAC}}\rangle\langle \tilde{0}|Q_N|\Psi_{\mathrm{SAC}}\rangle \tag{23}$$

and

$$\Delta V_{\mathrm{SAC}} = \langle \Lambda|V_N|\Psi_{\mathrm{SAC}}\rangle - \langle \Lambda'|\Psi_{\mathrm{SAC}}\rangle\langle \tilde{0}|V_N|\Psi_{\mathrm{SAC}}\rangle, \tag{24}$$

where Q_N and V_N are the normal ordered form of the apparent charges operator and of the electrostatic potential operator, respectively,

$$Q_N = Q - \mathbf{Q}_{\mathrm{HF}} \tag{25}$$

and

$$V_N = V - \mathbf{V}_{\mathrm{HF}}. \tag{26}$$

$\mathbf{V}_{\mathrm{HF}}$ is a vector collecting the HF values of the electrostatic potential generated by the solute at the sites of the polarization charges.[48,54]

The Hamiltonian matrix form of the PCM-SAC free-energy functional $L_{\mathrm{SAC}}^{\mathrm{PCM}}$ may simply be written as

$$L_{\mathrm{PCM}}^{\mathrm{SAC}} = \sum_I C_I \bar{H}_{0I}^{\mathrm{HF}}(1-\tilde{S}) + \sum_K Z_K\left(H_{K0}^{\mathrm{HF}} + \sum_I C_I \bar{H}_{KI}^{\mathrm{HF}}\right) + \frac{1}{2}\Delta Q_{\mathrm{SAC}}\cdot\Delta V_{\mathrm{SAC}}, \tag{27}$$

where the overlap $\tilde{S}$ has been defined in Eq. (9) and H_{IJ}^{HF} are the matrix elements of the Hamiltonian H_N^{HF},

$$H_{IJ}^{\mathrm{HF}} = \langle \tilde{0}|S_I H_N^{\mathrm{HF}} S_J^{\dagger}|\tilde{0}\rangle \quad \text{and} \quad H_{I,JK}^{\mathrm{HF}} = \langle \tilde{0}|S_I H_N^{\mathrm{HF}} S_J^{\dagger} S_K^{\dagger}|\tilde{0}\rangle. \tag{28}$$

The SAC polarization charges ΔQ_{SAC} and the SAC electrostatic potential ΔV_{SAC} of Eqs. (23) and (24) may be written in the following operator matrix forms:

$$\Delta Q_{\mathrm{SAC}} = \sum_I C_I Q_{0I}(1-\tilde{S}) + \sum_K Z_K\left(Q_{K0} + \sum_I C_I \bar{Q}_{KI}\right) \tag{29}$$

and

$$\Delta V_{\mathrm{SAC}} = \sum_I C_I V_{0I}(1-\tilde{S}) + \sum_K Z_K\left(V_{K0} + \sum_I C_I \bar{V}_{KI}\right), \tag{30}$$

where the matrix elements Q_{IJ} and V_{IJ} are given by

$$Q_{IJ} = \langle \tilde{0}|S_I Q_N S_J^{\dagger}|\tilde{0}\rangle \quad \text{and} \quad V_{IJ} = \langle \tilde{0}|S_I V_N S_J^{\dagger}|\tilde{0}\rangle. \tag{31}$$

The overbar denotes transformed matrix elements with the same transformation law defined in Eq. (11).

C. The PCM-SAC equations

The equations for the ground-sate PCM-SAC vectors follow from the stationarity conditions of the free-energy functional $L_{\mathrm{SAC}}^{\mathrm{PCM}}$. To simplify the comparison with the SAC equations [Eqs. (12)–(14)] of Sec. II A, we will present the PCM-SAC equations both in the state vector driven form and in the Hamiltonian matrix form. The Hamiltonian matrix form has been used in the previous papers on SAC/SAC-CI and in the SAC-CI guide.[55] The state vector form may be convenient for comparison with what has been reported earlier on the CC energy functional. Let us now first consider the PCM-SAC equations in the state vector form. They are then converted into the Hamiltonian matrix form.

The stationarity of $L_{\mathrm{SAC}}^{\mathrm{PCM}}$ with respect to the Z coefficients gives the equation for the C coefficients of the right SAC vector $|\Psi_{\mathrm{SAC}}\rangle$, while the stationarity with respect to the excitation amplitudes C gives the equation for the Z amplitudes of the left SAC vector $\langle\Lambda'|$. In contrast to the case of isolated molecules, where the equations for the left and right SAC vectors are not coupled, the PCM-SAC equations are coupled and they must be solved iteratively.

The equation for the right vector $|\Psi_{\mathrm{SAC}}\rangle$ is given by

$$\langle \tilde{0}|S_K(H_N^{\mathrm{PCM}} - \Delta E_{\mathrm{SAC}}^{\mathrm{PCM}})|\Psi_{\mathrm{SAC}}\rangle = 0, \tag{32}$$

where H_N^{PCM} is the PCM-SAC Hamiltonian for the solute and $\Delta E_{\mathrm{SAC}}^{\mathrm{PCM}}$ is the corresponding correlation energy. Equation (32) corresponds to the left-projection of the SAC expanded Schrödinger equation for the molecular solute

$$H_N^{\mathrm{PCM}}|\Psi_{\mathrm{SAC}}\rangle = \Delta E_{\mathrm{SAC}}^{\mathrm{PCM}}|\Psi_{\mathrm{SAC}}\rangle, \tag{33}$$

with

$$H_N^{\mathrm{PCM}} = H_N^{\mathrm{HF}} + (\langle \Lambda|Q_N|\Psi_{\mathrm{SAC}}\rangle - \langle \Lambda'|\Psi_{\mathrm{SAC}}\rangle\langle \tilde{0}|Q_N|\Psi_{\mathrm{SAC}}\rangle)\cdot V_N \tag{34}$$

and

$$\Delta E_{\mathrm{SAC}}^{\mathrm{PCM}} = \langle \tilde{0}|H_N^{\mathrm{PCM}}|\Psi_{\mathrm{SAC}}\rangle. \tag{35}$$

The first term of the PCM-SAC Hamiltonian H_N^{PCM} describes the solute in the presence of fixed HF polarization charges, while the second term represents the interaction of the solute with the SAC component of the polarization charges ΔQ_{SAC} [see Eq. (23)]. This last term introduces a dependence of H_N^{PCM} on both the left and right SAC vectors. As a consequence, the PCM-SAC Hamiltonian H_N^{PCM} is nonlinear, as expected for QM continuum solvation models,[11] and the SAC equation for the right vector is coupled with the corresponding equation for the left SAC vector. The Z-SAC equation for the left vector $\langle\Lambda'|$ is given by

$$\langle \Lambda|H_N^{\mathrm{PCM}} S_K^{\dagger}|\Psi_{\mathrm{SAC}}\rangle - \langle \Lambda'|S_K^{\dagger}|\Psi_{\mathrm{SAC}}\rangle\langle \tilde{0}|H_N^{\mathrm{PCM}}|\Psi_{\mathrm{SAC}}\rangle + \langle \Lambda'|\Psi_{\mathrm{SAC}}\rangle\langle \tilde{0}|H_N^{\mathrm{PCM}} S_K^{\dagger}|\Psi_{\mathrm{SAC}}\rangle = 0. \tag{36}$$

The equation may be easily compared with the corresponding Z-SAC equations for isolated molecules [see Eq. (7)].

The PCM-SAC equations in the Hamiltonian matrix form are considered in the same manner as those of isolated molecules. The PCM-SAC equations for the right SAC vector may be written as follows:

$$H_{K0}^{\mathrm{PCM}} + \sum_I C_I(\bar{H}_{KI}^{\mathrm{PCM}} - \bar{S}_{KI}\Delta E_{\mathrm{SAC}}^{\mathrm{PCM}}) = 0, \tag{37}$$

where H_{K0}^{PCM} are matrix elements of the PCM-SAC Hamiltonian (34) and $\Delta E_{\mathrm{SAC}}^{\mathrm{PCM}}$ is the correlation energy, hence

$$H_{KI}^{\mathrm{PCM}} = H_{KI}^{\mathrm{HF}} + \left[\sum_J C_J Q_{0J}(1-\tilde{S}) + \sum_K Z_K \left(Q_{K0} + \sum_J C_J \bar{Q}_{KJ} \right) \right] \cdot V_{KI} \tag{38}$$

and

$$\Delta E_{\mathrm{SAC}}^{\mathrm{PCM}} = \sum_I C_I \bar{H}_{0I}^{\mathrm{PCM}}, \tag{39}$$

where the overbar denotes a transformed matrix element according to Eq. (11). The PCM-SAC equations for the left SAC vector may be written as follows:

$$\bar{\bar{H}}_{0I}^{\mathrm{PCM}} + \sum_K Z_K Y_{KI}^{\mathrm{PCM}} + \sum_{KL} Z_K Z_L W_{KLI} = 0. \tag{40}$$

Detail of the expressions matrix elements $\bar{\bar{H}}_{0I}^{\mathrm{PCM}}$, Y_{KI}^{PCM}, and W_{KLI} are given in the Appendix. The PCM-SAC equations (37)–(40) show explicitly that they are coupled to obtain the C amplitudes for the right SAC vector from Eq. (37). We also have to determine the Z amplitudes for left SAC vectors from Eq. (40) and vice versa.

D. Analytical gradients of the PCM-SAC free-energy functional

The analytical gradients of the PCM-SAC free-energy functional $L_{\mathrm{SAC}}^{\mathrm{PCM},a} = \partial L_{\mathrm{SAC}}^{\mathrm{PCM}} / \partial a$ may be obtained by exploiting its stationary properties. To facilitate the relationship to the SAC gradients for isolated molecules we will present the PCM-SAC analytical gradients both in the Hamiltonian matrix form and in the MO integral-driven form. The Hamiltonian matrix form of the analytical gradients may be written as follows:

$$L_{\mathrm{SAC}}^{\mathrm{PCM},a} = \sum_I C_I H_{0I}^{\mathrm{HF},a}\tilde{S} + \sum_K \left(Z_K H_{K0}^{\mathrm{HF},a} + \sum_I C_I \bar{H}_{KI}^{\mathrm{HF},a} \right) + \frac{1}{2}(\Delta Q_{\mathrm{SAC}}^a \Delta V_{\mathrm{SAC}} + \Delta Q_{\mathrm{SAC}} \Delta V_{\mathrm{SAC}}^a), \tag{41}$$

where superscript a denotes differentiation with respect to the perturbing parameter a. The differentiated quantities $\Delta Q_{\mathrm{SAC}}^a$ and $\Delta V_{\mathrm{SAC}}^a$ are given by

$$\Delta Q_{\mathrm{SAC}}^a = \sum_I C_I Q_{0I}^a (1-\tilde{S}) + \sum_K Z_K \left(Q_{K0}^a + \sum_I C_I \bar{Q}_{KI}^a \right) \tag{42}$$

and

$$\Delta V_{\mathrm{SAC}}^a = \sum_I C_I V_{0I}^a (1-\tilde{S}) + \sum_K Z_K \left(V_{K0}^a + \sum_I C_I \bar{V}_{KI}^a \right). \tag{43}$$

The PCM-SAC gradients may be written in terms of the derivatives of the MO integrals as follows:

$$L_{\mathrm{SAC}}^{\mathrm{PCM},a} = \sum_{rs}^{\mathrm{MO}} \gamma_{rs}^{\mathrm{SAC}} f_{rs}^{\mathrm{PCM},a} + \sum_{rstu}^{\mathrm{MO}} \Gamma_{rstu}^{\mathrm{SAC}} (rs|tu)^a + \frac{1}{2} \sum_{rs}^{\mathrm{MO}} \sum_{tu}^{\mathrm{MO}} \gamma_{rs}^{\mathrm{SAC}} \gamma_{tu}^{\mathrm{SAC}} (q_{rs}^a v_{tu} + q_{rs} v_{tu}^a), \tag{44}$$

where γ^{SAC} and Γ^{SAC} are elements of the SAC one- and two-particle density matrices, respectively.[16] For the evaluation of the PCM-SAC gradient Lagrangian we need the first derivatives of the PCM-Fock matrix $f_{rs}^{\mathrm{PCM},a}$ and of the PCM one-electron operators q_{rs}^a and v_{tu}^a.[56] These derivative of MO integrals lead to two types of terms: one involving the skeleton derivative of the corresponding AO (atomic orbital) integrals and the other involving the derivatives of the MO coefficients.

The MO integral form of the PCM-SAC gradients may be written as follows:

$$\begin{aligned} L_{\mathrm{SAC}}^{\mathrm{PCM},a} = & \sum_{ij}^{\mathrm{occ}} \gamma_{ij}^{\mathrm{SAC}} f_{ij}^{\mathrm{PCM},[a]} + \sum_{ab}^{\mathrm{vac}} \gamma_{ab}^{\mathrm{SAC}} f_{ab}^{\mathrm{PCM},[a]} \\ & + \sum_{pq}^{\mathrm{MO}} \gamma_{pq}^{\mathrm{SAC}} v_{pq}^{[a]} \Delta Q_{\mathrm{SAC}} + \sum_{pqrs}^{\mathrm{MO}} \Gamma_{pqrs}^{\mathrm{SAC}} (pq|rs)^{[a]} \\ & - \sum_{ij}^{\mathrm{occ}} S_{ij}^{[a]} X_{ij}^{\mathrm{PCM}} - \sum_{ab}^{\mathrm{vac}} S_{ab}^{[a]} X_{ab}^{\mathrm{PCM}} + 2 \sum_{i}^{\mathrm{occ}} \sum_{a}^{\mathrm{vac}} S_{ai}^{[a]} X_{ai}^{\mathrm{PCM}} \\ & + 2 \sum_{i}^{\mathrm{occ}} \sum_{a}^{\mathrm{vac}} U_{ai}^a (X_{ai}^{\mathrm{PCM}} - X_{ia}^{\mathrm{PCM}}), \end{aligned} \tag{45}$$

where the superscript $[a]$ denotes the skeleton derivatives of the pertinent AO integrals, U_{ai}^a are the derivative of the MO coefficients in the MO basis, and the matrix elements $X_{t,p}^{\mathrm{PCM}}$ are given by

$$\begin{aligned} X_{t,p}^{\mathrm{PCM}} = & \sum_{q}^{\mathrm{MO}} \gamma_{pq}^{\mathrm{SAC}} f_{tq}^{\mathrm{PCM}} (\delta_{pi}\delta_{qj} + \delta_{pa}\delta_{qb}) + 2 \sum_{qrs}^{\mathrm{MO}} \Gamma_{pqrs} (tq|rs) \\ & + \frac{1}{2} \sum_{rs}^{oo/vv} (A_{tp,rs} + \mathcal{B}_{tp,rs}) \delta_{ti} \gamma_{rs}^{\mathrm{SAC}} \\ & + \sum_{q}^{\mathrm{MO}} \gamma_{pq}^{\mathrm{SAC}} v_{tq}^a \Delta Q_{\mathrm{SAC}}, \end{aligned} \tag{46}$$

where $A_{tp,rs}$ is a linear combination of the two-electron integral defined in Ref. 57.

An explicit solution of the derivative of the MO coefficient U_{ai}^a can be avoided by using the interchange technique for the PCM model,[51,56]

$$\sum_{ai} Y_{ai}^{\mathrm{PCM}} U_{ai}^{\alpha} = \sum_{ai} \gamma_{ai}^{\mathrm{MO\text{-}resp}} Q_{ai}^{\mathrm{PCM},\alpha}, \tag{47}$$

where $Y_{ai}^{\mathrm{PCM}} = X_{ai}^{\mathrm{PCM}} - X_{ia}^{\mathrm{PCM}}$. Here $\gamma_{ai}^{\mathrm{MO\text{-}resp}}$ is the vacant-occupied block of the orbital response contribution to the one-particle density matrix, and the matrix elements Q_{ai}^{α} are given by Refs. 17, 58, and 13,

$$Q_{ai}^{\mathrm{PCM},\alpha} = f_{ai}^{\mathrm{PCM},[\alpha]} - S_{ai}^{\alpha} f_{ii}^{\mathrm{PCM}} - \sum_{kl} S_{kl}^{[\alpha]} [A_{ai,kl} + \mathcal{B}_{ai,kl}]. \tag{48}$$

The matrix elements $\gamma_{ai}^{\mathrm{MO\text{-}resp}}$ are obtained as the solution to a linear system of equations that are independent from the perturbation. The final expression of the PCM-SAC gradients may be then written as follows:

$$\begin{aligned} L_{\mathrm{SAC}}^{\mathrm{PCM},a} = & \sum_{ij}^{\mathrm{occ}} \gamma_{ij}^{\mathrm{SAC}} f_{ij}^{\mathrm{PCM},[a]} + \sum_{ab}^{\mathrm{vac}} \gamma_{ab}^{\mathrm{SAC}} f_{ab}^{\mathrm{PCM},[a]} \\ & + 2 \sum_{i}^{\mathrm{occ}} \sum_{a}^{\mathrm{vac}} \gamma_{ai}^{\mathrm{MO\text{-}resp}} f_{ai}^{\mathrm{PCM},[a]} + \sum_{pq}^{\mathrm{MO}} \gamma_{pq}^{\mathrm{SAC}} v_{pq}^{[a]} \Delta Q_{\mathrm{SAC}} \\ & + \sum_{pqrs}^{\mathrm{MO}} \Gamma_{pqrs}^{\mathrm{SAC}} (pq|rs)^{[a]} - \sum_{ij}^{\mathrm{occ}} \tilde{S}_{ij}^{[a]} X_{ij}^{\mathrm{PCM}} \\ & - \sum_{ab}^{\mathrm{vac}} S_{ab}^{[a]} X_{ab}^{\mathrm{PCM}} + 2 \sum_{i}^{\mathrm{occ}} \sum_{a}^{\mathrm{vac}} S_{ai}^{[a]} \tilde{X}_{ai}^{\mathrm{PCM}}, \end{aligned} \tag{49}$$

where $\tilde{X}_{ai}^{\mathrm{PCM}} = X_{ai}^{\mathrm{PCM}} - \gamma_{ai}^{\mathrm{MO\text{-}resp}} f_{ii}$. $\tilde{X}_{ij}^{\mathrm{PCM}}$ is defined by

$$\tilde{X}_{ij}^{\mathrm{PCM}} = X_{ij}^{\mathrm{PCM}} - 2 \sum_{em} \gamma_{em}^{\mathrm{MO\text{-}resp}} (A_{ij,em} + \mathcal{B}_{ij,em}). \tag{50}$$

The PCM-SAC analytical gradients of Eq. (49) complete the description of the PCM-SAC theory for the ground state of solvated molecules. An alternative derivation of the PCM-SAC energy gradients is possible by considering the Lagrange multiplier for orbital rotation.[14] The aspects concerning the implementation of the theory in a computational QM code will be discussed in Sec. III. A parallel discussion for the excited states (PCM-SAC-CI) is now presented in the following subsections.

E. The SAC-CI theory: An energy functional approach

Here we review a formulation of SAC-CI based on an energy functional approach. Using the same motivation as for the SAC theory, we will present both the state vector and the Hamiltonian matrix formalism. The SAC-CI wave functions for excited states are defined in the functional space complementary to the SAC wave function $|\Psi_{\mathrm{SAC}}\rangle$. The basis of this space is given by a selected set of linked excitations from the SAC ground state.

In the SAC-CI energy functional approach we consider three SAC-CI vectors for each electronic state: a right SAC-CI vector, $|\Psi_{\mathrm{SACCI}}\rangle$, a left SAC-CI vector, $\langle\Psi_{\mathrm{SACCI}}|$ and an auxiliary SAC-CI left vector $\langle\Lambda''|$. The right SAC-CI vector $|\Psi_{\mathrm{SACCI}}\rangle$ is written as

$$|\Psi_{\mathrm{SACCI}}\rangle = R^{p}|\Psi_{\mathrm{SAC}}\rangle \quad \text{and} \quad R^{p} = \sum_{M} d_{M}^{R,p} R_{M}^{\dagger}, \tag{51}$$

where the superscript p denotes a generic pth excited state and where $R_M^{\dagger}$ denotes a set of excitation operators. The left SAC-CI vector $\langle\Psi_{\mathrm{SACCI}}|$ is given by

$$\langle\Psi_{\mathrm{SACCI}}^{L}| = \langle\Psi_{\mathrm{SAC}}|L^{p} \quad \text{and} \quad L^{p} = \sum_{M} d_{M}^{L,p} R_{M}, \tag{52}$$

where R_M denotes a set of de-excitation operators. The auxiliary left SAC-CI vector $\langle\Lambda''|$ is defined as

$$\langle\Lambda''| = \sum_{K} Z_{K}^{\mathrm{SACCI}} \langle 0|S_{K}, \tag{53}$$

where S_M is a de-excitation operator introduced in Eq. (2). The sets of the SAC-CI coefficients, d^R, d^L and Z^{SACCI}, are determined from the stationarity conditions of the SAC-CI energy functional, with the additional constraint of the biorthogonality between the left and right SAC vectors

$$\langle\Psi_{\mathrm{SACCI}}^{L}|\Psi_{\mathrm{SACCI}}^{R}\rangle = 1. \tag{54}$$

The SAC-CI energy functional may be defined as

$$\begin{aligned} L_{\mathrm{SACCI}} = & \langle\Psi_{\mathrm{SACCI}}^{L}|H_{N}|\Psi_{\mathrm{SACCI}}^{R}\rangle + \langle\Lambda''|H_{N}|\Psi_{\mathrm{SAC}}\rangle \\ & - \langle\Lambda''|\Psi_{\mathrm{SAC}}\rangle\langle 0|H_{N}|\Psi_{\mathrm{SAC}}\rangle, \end{aligned} \tag{55}$$

where H_N is the normal ordered Hamiltonian. The stationarity of L_{SACCI} with respect to the R_M amplitudes gives the equation for the right SAC-CI vector, while the stationarity with respect to the L_M amplitudes leads to the equation for the left SAC-CI vector. Specifically, the equation for the right SAC-CI vector corresponds to the projection of the right SAC-CI Schrödinger equation,[4,5]

$$H_{N}|\Psi_{\mathrm{SACCI}}^{R}\rangle = \Delta E_{\mathrm{SACCI}}|\Psi_{\mathrm{SACCI}}^{R}\rangle, \tag{56}$$

where $\Delta E_{\mathrm{SACCI}}$ is given by

$$\Delta E_{\mathrm{SACCI}} = \langle\Psi_{\mathrm{SACCI}}^{L}|H_{N}|\Psi_{\mathrm{SACCI}}^{R}\rangle. \tag{57}$$

The equation for the left SAC-CI vector corresponds to the projection of the left SAC-CI Schrödinger equation,

$$\langle\Psi_{\mathrm{SACCI}}^{L}|\Delta E_{\mathrm{SACCI}} = \langle\Psi_{\mathrm{SACCI}}^{L}|H_{N}. \tag{58}$$

The stationarity of L_{SACCI} with respect to the Z_K amplitudes leads to the equation for the SAC state [see Eq. (5)], while the stationarity of L_{SACCI} with respect to the C_K amplitudes gives the equations for the amplitudes of the left vector $\langle\Lambda''|$ [see Eq. (64) below].

The SAC-CI energy functional may be expressed in the Hamiltonian matrix form as follows:

$$\begin{aligned} L_{\mathrm{SACCI}} = & \sum_{MN} d_{M}^{L,p} d_{M}^{R,p} \bar{\bar{H}}_{MN} + \sum_{K} Z_{K} H_{K0} + \sum_{KI} Z_{K} C_{I} \bar{H}_{KI} \\ & - \sum_{KI} Z_{K} C_{I} \bar{S}_{KI} \sum_{J} C_{J} \bar{H}_{0J}, \end{aligned} \tag{59}$$

where $d_M^{L,p}$ and $d_M^{R,p}$ are the left- and right vector coefficients for the pth solution of the SAC-CI equations (56)–(58). We adopt the convention that the subscripts I, J, K, and L refer to the SAC excitation operators, while M and N refer to the

SAC-CI operators. The left and right SAC-CI vectors satisfy a biorthonormalization condition

$$\sum_{MN} d_M^{L,p} d_M^{R,p} \bar{\bar{S}}_{MN} = 1, \tag{60}$$

where $\bar{\bar{S}}_{MN} = S_{MN} + \Sigma_J C_J S_{M,NJ}$.

The Hamiltonian form of the SAC-CI equations (56)–(58) may be written, respectively, as

$$\sum_N d_N^R [\bar{\bar{H}}_{MN} - \Delta E_{\mathrm{SACCI}} \bar{\bar{S}}_{MN}] = 0, \tag{61}$$

$$\Delta E_{\mathrm{SACCI}} = \sum_{MN} d_M^{L,p} d_M^{R,p} \bar{\bar{H}}_{MN}, \tag{62}$$

and

$$\sum_M d_M^L [\bar{\bar{H}}_{MN} - \Delta E_{\mathrm{SACCI}} \bar{\bar{S}}_{MN}] = 0. \tag{63}$$

The corresponding SAC-CI equation for the Z amplitudes is given by

$$\bar{\bar{H}}_I + \sum_L Z_L^{\mathrm{SAC}} Y_{IL} = 0, \tag{64}$$

where the matrix elements $\bar{\bar{H}}_I$ are given by

$$\bar{\bar{H}}_I = \sum_{MN} d_M^L d_N^R (H_{M,NI} - \Delta E_{\mathrm{SACCI}} S_{M,NI}). \tag{65}$$

Equation (64) corresponds to the Z-SAC-CI equation given in Ref. 16.

When the stationary conditions are satisfied the SAC-CI energy functional reduces to the SAC energy, i.e., $L_{\mathrm{SACCI}} = \Delta E_{\mathrm{SACCI}}$, and the analytical gradients of $\Delta E_{\mathrm{SACCI}}$ can be determined as analytical gradients of L_{SACCI}. The analytical gradients $L^a_{\mathrm{SACCI}} = \partial L_{\mathrm{SACCI}} / \partial a$ with respect to a perturbation parameter a can be written in the following Hamiltonian matrix form:

$$L^a_{\mathrm{SACCI}} = \sum_{MN} d_M^{L,p} d_M^{R,p} \bar{\bar{H}}^a_{MN} + \sum_K Z_K H^a_{K0} + \sum_{KI} Z_K C_I \bar{H}^a_{KI} - \sum_{KI} Z_K C_I \bar{S}_{KI} \sum_J C_J \bar{H}^a_{0J}, \tag{66}$$

where the superscript a denotes differentiation of the corresponding Hamiltonian matrix elements. Equation (66) is equivalent to the expression of the analytical gradient of the SAC-CI correlation energy given in Ref. 16. The derivatives of the Hamiltonian matrix elements appearing in Eq. (66) may be expressed in terms of derivatives of the Fock matrix elements and of the two-electron repulsion integrals. The computationally demanding evaluation of the MO derivative terms may be avoided by exploiting the interchange theorem approach.[53] The gradient equation (66) completes our presentation of the SAC-CI theory for isolated molecules based on the energy functional approach. The PCM-SAC-CI energy functional is introduced in the following subsection.

F. PCM-SAC-CI free-energy functional

The PCM-SAC-CI wave functions for excited states of solvated molecules are defined to belong to the functional space complementary to the SAC ground state, determined in the presence of the fixed HF reaction field. The PCM-SAC-CI vectors are defined accordingly as follows:

$$|\Psi_{\mathrm{SACCI}}\rangle = R^p |\Psi_{\mathrm{SAC}}(0)\rangle, \quad R^p = \sum_M d_M^p R_M^\dagger, \tag{67}$$

$$\langle \Psi^L_{\mathrm{SACCI}}| = \langle \Psi_{\mathrm{SAC}}(0)| L^p, \quad L^p = \sum_M d_M^p R_M, \tag{68}$$

and

$$\langle \Lambda''| = \sum_K Z_K^{\mathrm{SACCI}} \langle \tilde{0}| S_K, \tag{69}$$

where $|\tilde{0}\rangle$ is the HF state of the molecular solute and $|\Psi_{\mathrm{SAC}}(0)\rangle$ is the SAC wave function that satisfies the SAC equation,

$$\langle \tilde{0}| S_K H_N^{\mathrm{HF}} |\Psi_{\mathrm{SAC}}(0)\rangle - \langle \tilde{0}| S_K |\Psi_{\mathrm{SAC}}(0)\rangle \langle \tilde{0}| H_N^{\mathrm{HF}} |\Psi_{\mathrm{SAC}}\rangle = 0, \tag{70}$$

where H_N^{HF} is the Hamiltonian in the presence of the fixed HF polarization charges [see Eq. (21)]. The PCM-SAC-CI free-energy functional may be written as

$$L^{\mathrm{PCM}}_{\mathrm{SACCI}} = \langle \Psi^{L,p}_{\mathrm{SACCI}} | H_N^{\mathrm{HF}} | \Psi^{R,p}_{\mathrm{SACCI}} \rangle - \langle \Lambda'' | H_N^{\mathrm{HF}} | \Psi_{\mathrm{SAC}} \rangle - \langle \Lambda'' | \Psi_{\mathrm{SAC}} \rangle \langle \tilde{0} | H_N^{\mathrm{HF}} | \Psi_{\mathrm{SAC}} \rangle + \tfrac{1}{2} \Delta Q_{\mathrm{SACCI}} \Delta V_{\mathrm{SACCI}}, \tag{71}$$

where $\Delta Q_{\mathrm{SACCI}}$ and $\Delta V_{\mathrm{SACCI}}$ are the SAC-CI expectation values of the polarization charges and of the electrostatic potential operators, respectively. The first two terms in a SAC-CI free-energy functional represent an excited electronic state in the presence of the HF polarization charges, while the third term represents the SAC-CI contribution to the solute-solvent interaction. The SAC-CI expectation values $\Delta Q_{\mathrm{SACCI}}$ and $\Delta V_{\mathrm{SACCI}}$ may be written as

$$\Delta Q_{\mathrm{SACCI}} = \langle \Psi^{L,p}_{\mathrm{SACCI}} | Q_N | \Psi^{R,p}_{\mathrm{SACCI}} \rangle \tag{72}$$

and

$$\Delta V_{\mathrm{SACCI}} = \langle \Psi^{L,p}_{\mathrm{SACCI}} | V_N | \Psi^{R,p}_{\mathrm{SACCI}} \rangle. \tag{73}$$

The Hamiltonian matrix form of the PCM-SAC-CI free-energy functional is given by

$$L^{\mathrm{PCM}}_{\mathrm{SACCI}} = \sum_{MN} d_M^{L,p} d_M^{R,p} \bar{\bar{H}}^{\mathrm{HF}}_{MN} + \sum_K Z_K H^{\mathrm{HF}}_{K0} + \sum_{KI} Z_K C_I \bar{H}^{\mathrm{HF}}_{KI} - \sum_{KI} Z_K C_I \bar{S}_{KI} \sum_J C_J \bar{H}^{\mathrm{HF}}_{0J} + \left(\sum_{MN} d_M^{L,p} d_M^{R,p} \bar{\bar{V}}_{MN} \right) \times \left(\sum_{MN} d_M^{L,p} d_M^{R,p} \bar{\bar{Q}}_{MN} \right), \tag{74}$$

where we have introduced the transformed matrix elements

$$\bar{\bar{Q}}_{MN} = Q_{MN} + \sum_J C_J Q_{M,NJ} \tag{75}$$

and

$$\bar{\bar{V}}_{MN} = V_{MN} + \sum_J C_J V_{M,NJ}. \tag{76}$$

G. The PCM-SAC-CI equations

The PCM-SAC-CI equations may be obtained from the stationarity of the free-energy functional $L^{\mathrm{PCM}}_{\text{SAC-CI}}$. The stationarity of $L^{\mathrm{PCM}}_{\mathrm{SACCI}}$ with respect to the R_K and L_K amplitudes leads, respectively, to the projection of the right and left SAC-CI Schrödinger equation

$$H_N^{\mathrm{PCM},p}|\Psi^R_{\mathrm{SACCI}}\rangle = \Delta E^{\mathrm{PCM}}_{\mathrm{SACCI}}|\Psi^R_{\mathrm{SACCI}}\rangle \tag{77}$$

and

$$\langle\Psi^L_{\mathrm{SACCI}}|\Delta E^{\mathrm{PCM}}_{\mathrm{SACCI}} = \langle\Psi^L_{\mathrm{SACCI}}|H_N^{\mathrm{PCM},p}, \tag{78}$$

where the PCM-SAC-CI energy $\Delta E^{\mathrm{PCM}}_{\mathrm{SACCI}}$ is given by

$$\Delta E^{\mathrm{PCM}}_{\mathrm{SACCI}} = \langle\Psi^L_{\mathrm{SACCI}}|H_N^{\mathrm{PCM},p}|\Psi^R_{\mathrm{SACCI}}\rangle \tag{79}$$

and $H_N^{\mathrm{PCM},p}$ is the PCM-SAC-CI Hamiltonian for the solute in the pth excited state of interest

$$H_N^{\mathrm{PCM},p} = H_N^{\mathrm{HF}} + \Delta Q_{\mathrm{SACCI}} V_N. \tag{80}$$

The stationarity of $L^{\mathrm{PCM}}_{\mathrm{SACCI}}$ with respect to the Z_K amplitudes gives the PCM-SAC equation (37), while the stationarity of $L^{\mathrm{PCM}}_{\mathrm{SACCI}}$ with respect to the C_K amplitudes gives the SAC-CI equation for the amplitudes of the auxiliary left vector [see Eq. (84) later].

The Hamiltonian matrix form of the PCM-SAC-CI equations (77)–(79) may be written, respectively, as

$$\sum_N d_N^R[\bar{\bar{H}}^{\mathrm{PCM},p}_{MN} - \Delta E^{\mathrm{PCM}}_{\mathrm{SACCI}}\bar{\bar{S}}_{MN}] = 0, \tag{81}$$

$$\sum_M d_M^L[\bar{\bar{H}}^{\mathrm{PCM},p}_{MN} - \Delta E^{\mathrm{PCM}}_{\mathrm{SACCI}}\bar{\bar{S}}_{MN}] = 0, \tag{82}$$

and

$$\Delta E^{\mathrm{PCM},p}_{\mathrm{SACCI}} = \sum_{MN} d_M^{L,p} d_N^{R,p} \bar{\bar{H}}^{\mathrm{PCM},p}_{MN}. \tag{83}$$

The corresponding equation for the Z amplitudes is given by

$$\frac{\partial L_{\mathrm{SACCI}}}{\partial C_I} = \bar{\bar{H}}_I(\mathrm{PCM},p) + \sum_L Z_L^{\mathrm{SAC}} Y_{IL}^{\mathrm{HF}} = 0, \tag{84}$$

where the Hamiltonian matrix integrals $\bar{\bar{H}}^{\mathrm{PCM},p}_{MN}$ refers to the PCM-SAC-CI Hamiltonian (80), and the matrix integral $\bar{\bar{H}}_I(\mathrm{PCM})$ of Eq. (84) is given by

$$\bar{\bar{H}}_I(\mathrm{PCM},p) = \sum_{MN} d_M^L d_N^R (H^{\mathrm{PCM},p}_{M,NI} - \Delta E^{\mathrm{PCM},p}_{\mathrm{SACCI}} S_{M,NI}). \tag{85}$$

H. PCM-SAC-CI analytical gradients

The first derivative of the PCM-SAC energy functional $L^{\mathrm{PCM}}_{\mathrm{SACCI}}$ may be easily obtained by exploiting the stationary conditions described in the previous subsection. To simplify the relationship with the SAC-CI gradients for isolated molecules,[16] we will present the PCM-SAC gradients both in the Hamiltonian matrix form and in the MO integrals driven form.

The analytical gradients of $L^{\mathrm{PCM},a}_{\mathrm{SACCI}} = \partial L^{\mathrm{PCM},p}_{\mathrm{SACCI}}/\partial a$ may be written as

$$\begin{aligned} L^{\mathrm{PCM},a}_{\mathrm{SACCI}} &= \sum_{MN} d_M^{L,p} d_N^{R,p} \bar{\bar{H}}^a_{MN} \\ &+ \frac{1}{2}\sum_{MN}\sum_{M'N'} d_M^{L,p} d_N^{R,p} d_{M'}^{L,p} d_{N'}^{R,p} (\bar{\bar{Q}}^a_{MN}\bar{\bar{V}}_{M'N'} \\ &+ \bar{\bar{Q}}_{M'N'}\bar{\bar{V}}^a_{MN}) + \sum_K Z_K H^{\mathrm{HF},a}_{K0} + \sum_{KI} Z_K C_I \bar{H}^{\mathrm{HF},a}_{KI} \\ &- \sum_{KI} Z_K C_I \bar{S}_{KI} \sum_J C_J \bar{H}^{\mathrm{HF},a}_{0J}, \end{aligned} \tag{86}$$

where the superscript a denotes differentiation of the pertinent matrix elements. In terms of the differentiated MO integrals, the analytical gradients $L^{\mathrm{PCM},a}_{\mathrm{SACCI}}$ may be written in a form similar to the corresponding PCM-SAC gradients of Eq. (44), namely,

$$\begin{aligned} L^{\mathrm{PCM},a}_{\mathrm{SACCI}} &= \sum_{ij}^{\mathrm{occ}} \gamma^{\mathrm{SACCI}}_{ij} f^{\mathrm{PCM},a}_{ij} + \sum_{ab}^{\mathrm{vac}} \gamma^{\mathrm{SACCI}}_{ab} f^{\mathrm{PCM},a}_{ab} \\ &+ \sum_{pq}^{\mathrm{MO}} \gamma^{\mathrm{SACCI,NR}}_{pq} v^a_{pq} \Delta Q_{\mathrm{SAC}} + \sum_{pqrs}^{\mathrm{MO}} \Gamma^{\mathrm{SACCI}}_{pqrs} (pq|rs)^a \\ &- \sum_{ij}^{\mathrm{occ}} S^a_{ij} X^{\mathrm{PCM},p}_{ij} - \sum_{ab}^{\mathrm{vac}} S^a_{ab} X^{\mathrm{PCM},p}_{ab} \\ &+ 2\sum_i^{\mathrm{occ}}\sum_a^{\mathrm{vac}} S^a_{ai} X^{\mathrm{PCM},p}_{ai} + 2\sum_i^{\mathrm{occ}}\sum_a^{\mathrm{vac}} U^a_{ai} Y^{\mathrm{PCM},p}_{ai}, \end{aligned} \tag{87}$$

where $\gamma^{\mathrm{SACCI}}_{ij}$ and $\gamma^{\mathrm{SACCI,NR}}_{ij}$ are the SAC-CI one-particle density matrix and its nonrelaxed components,[16] respectively, matrix elements $X^{\mathrm{PCM},p}_{t,p}$ are given by

$$\begin{aligned} X^{\mathrm{PCM},p}_{t,p} &= \sum_q^{MO} \gamma^{\mathrm{SACCI}}_{pq} f^{\mathrm{PCM}}_{tq} (\delta_{pi}\delta_{qj} + \delta_{pa}\delta_{qb}) \\ &+ 2\sum_{qrs}^{\mathrm{MO}} \Gamma^{\mathrm{SACCI}}_{pqrs}(tq|rs) + \frac{1}{2}\sum_{rs}^{oo/vv} (A_{tp,rs} \\ &+ \mathcal{B}_{tp,rs})\delta_{ti}\gamma^{\mathrm{SACCI}}_{rs} + \sum_q^{\mathrm{MO}} \gamma^{\mathrm{SACCI,NR}}_{pq} v^a_{tq} \Delta Q_{\mathrm{SACCI}} \end{aligned} \tag{88}$$

and $Y^{\mathrm{PCM},p}_{ai} = X^{\mathrm{PCM},p}_{ai} - X^{\mathrm{PCM},p}_{ia}$. The explicit solution of the derivative of the MO coefficient, U^a_{ai}, can be avoided by using the interchange technique for the PCM model,[53,58,13]

$$\sum_{ai} Y_{ai}^{\mathrm{PCM},p} U_{ai}^{\alpha} = \sum_{ai} \gamma_{ai}^{\mathrm{MO\text{-}resp}} Q_{ai}^{\mathrm{PCM},a}, \tag{89}$$

where $\gamma_{ai}^{\mathrm{MO\text{-}resp}}$ is the vacant-occupied block of the orbital response contribution to the one-particle density matrix. The matrix elements Q_{ai}^{α} are given in Ref. 17. The matrix elements $\gamma_{ai}^{\mathrm{MO\text{-}resp}}$ are obtained as the solution of a linear system of equations independent from the perturbation. The final expression of the analytical gradients $L_{\mathrm{SACCI}}^{\mathrm{PCM},a}$ may be written as

$$\begin{aligned} L_{\mathrm{SACCI}}^{\mathrm{PCM},a} = & \sum_{ij}^{\mathrm{occ}} \gamma_{ij}^{\mathrm{SACCI}} f_{ij}^{\mathrm{PCM},a} + \sum_{ab}^{\mathrm{vac}} \gamma_{ab}^{\mathrm{SACCI}} f_{ab}^{\mathrm{PCM},a} \\ & + 2 \sum_{i}^{\mathrm{occ}} \sum_{a}^{\mathrm{vac}} \gamma_{ai}^{\mathrm{MO\text{-}resp}} f_{ai}^{\mathrm{PCM},a} \\ & + \sum_{pq}^{\mathrm{MO}} \gamma_{pq}^{\mathrm{SACCI,NR}} v_{pq}^{a} \Delta Q_{\mathrm{SACCI}} \\ & + \sum_{pqrs}^{\mathrm{MO}} \Gamma_{pqrs}^{\mathrm{SACCI}} (pq|rs)^{a} - \sum_{ij}^{MO} \tilde{S}_{ij}^{a} X_{ij}^{\mathrm{PCM/SACCI}} \\ & - \sum_{ab}^{\mathrm{MO}} S_{ab}^{a} X_{ab}^{\mathrm{PCM/SACCI}} + 2 \sum_{ai}^{\mathrm{MO}} S_{ai}^{a} \tilde{X}_{ai}^{\mathrm{PCM/SACCI}}, \end{aligned} \tag{90}$$

where $\tilde{X}_{ai}^{\mathrm{PCM},p} = X_{ai}^{\mathrm{PCM},p} - \gamma_{ai}^{\mathrm{MO\text{-}resp}} f_{ii}$ and $\tilde{X}_{ij}^{\mathrm{PCM/SAC\text{-}CI}}$ is defined as

$$\tilde{X}_{ij}^{\mathrm{PCM},p} = X_{ij}^{\mathrm{PCM},p} - 2 \sum_{em} \gamma_{em}^{\mathrm{MO\text{-}resp}} (A_{jm,em} + \mathcal{B}_{ijem}). \tag{91}$$

The above analytical gradients complete the PCM-SAC-CI theory for the excited states of solvated molecules. Its implementation is discussed in Sec. III.

III. IMPLEMENTATION OF PCM IN THE SAC-CI PROGRAM

The PCM-SAC and PCM-SAC-CI theories presented in the above section were implemented in the latest version of the SAC-CI program in which the MO direct formulation and algorithm are used for practical calculations.[35,55] The direct SAC-CI method constructs iteration vectors from the MO integrals without using an explicit Hamiltonian matrix formula. A Hamiltonian matrix element can be written in the MO integral form as

$$H_{IJK} = \sum_{pq}^{\mathrm{MO}} g_{IJK}^{pq} f_{pq} + \sum_{pqrs}^{\mathrm{MO}} G_{IJK}^{pqrs} (pq|rs), \tag{92}$$

where g_{IJK}^{pq} and G_{IJK}^{pqrs} are the coupling constants. The PCM contributions are essentially one-electron operators. In practical computation, therefore, the additional terms are summed into the Fock matrix. This modified Fock matrix is computed using the SAC or SAC-CI density matrix and the program routine for PCM in GAUSSIAN.[50] The PCM-SAC/SAC-CI equations and the energy gradient formula are solved by considering the modified Fock matrix. The PCM-SAC/SAC-CI equations are nonlinear and are solved iteratively.

The PCM-SAC energy gradient calculation is summarized as follows:

(1) The PCM-SCF calculation is performed.
(2) A first guess of the SAC amplitudes is obtained by solving the PCM-SAC equation (38) by neglecting the Z-SAC coefficient.
(3) The PCM-Z-SAC equation (40) is solved using the SAC amplitudes obtained as described in the previous step. One of the Z-SAC vectors in the quadratic terms is fixed as the values in the previous iteration. The linearized equation is solved as

$$\bar{\bar{H}}_{0I}^{\mathrm{PCM}} + \sum_{K} Z_K \left(Y_{KI}^{\mathrm{PCM}} + \sum_{L} Z'_L W_{KLI} \right), \tag{93}$$

where $\{Z'_L\}$ was obtained by the previous iteration.
(4) The PCM-SAC equation (38) is solved using the SAC amplitudes and the Z-SAC coefficients obtained in the previous iteration.
(5) Steps 3 and 4 are repeated until convergence is reached. At convergence, $\{Z_K\}$ and $\{Z'_L\}$ are identical.
(6) The PCM-SAC free-energy is obtained by Eqs. (20) and (27).
(7) The final SAC effective density matrices are stored.
(8) The PCM-SAC geometrical gradients are computed using Eq. (45), avoiding the explicit solution of the MO coefficients by using the interchange technique.

The PCM-SAC-CI energy gradient calculation is summarized as follows:

(1) The PCM-SCF calculation is performed.
(2) The SAC equations are solved in the presence of the HF reaction field [see Eq. (21)].
(3) The PCM-SAC-CI Hamiltonian is formed using Eqs. (72) and (80) with a given initial vector (usually CIS wave function is used).
(4) The PCM-SAC-CI equations (81)–(83) are solved.
(5) The PCM-SAC-CI Hamiltonian is updated with the obtained PCM-SAC-CI wave function.
(6) Steps 4 and 5 are repeated until convergence is reached.
(7) The PCM-SAC-CI free-energy is obtained by Eqs. (79) and (83).
(8) The PCM-Z-SAC-CI equation (84) is solved using the SAC-CI amplitudes.
(9) The final SAC-CI effective density matrices are stored.

TABLE I. Typical computational routes for PCM SAC/SAC-CI computation.

Route	Electronic state	Geometry	Solvation
1	Ground	Ground	Equilibrium
2	Excited	Ground	Nonequilibrium
3	Excited	Excited	Equilibrium
4	Ground	Excited	Nonequilibrium
Energy difference	Transition		
ΔG(route 1,route 2)	Vertical absorption		
ΔG(route 1,route 3)	Adiabatic transition		
ΔG(route 3,route 4)	Vertical emission		

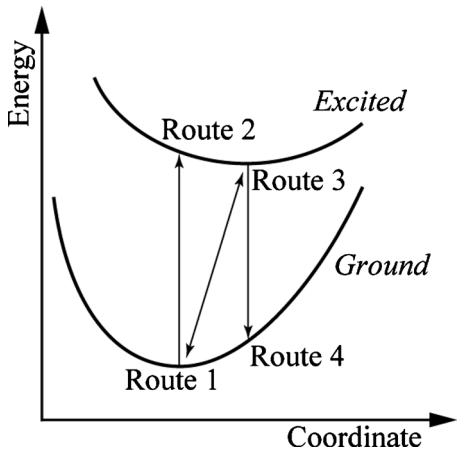

FIG. 1. Computational routes and transitions.

(10) The PCM-SAC-CI geometrical gradients are computed using Eq. (90), avoiding the explicit solution of the MO coefficients by using the interchange technique.

Many routines of GAUSSIAN are used for the parts related to the interchange technique, the coupled perturbed HF equations, and the gradient evaluation in the link 1111, link 1002, and overlay 7.[50]

IV. RESULTS AND DISCUSSIONS

A. Computational details

In studying the types of electronic transition between different states, there are four possible combinations of the electronic state, molecular geometry, and solvation model, as summarized in Table I and illustrated in Fig. 1. For the sake of clear discussion, the types of computation defined by Table I are named computational "routes," which represent electronic state, molecular geometry, and solvation model. The transitions between routes 1 and 2 and between routes 3 and 4 correspond to vertical absorption and emission, respectively. The transition between routes 1 and 3 is an adiabatic one. For the emission process, the excited state must be considered as the initial state of nonequilibrium solvation in route 4; therefore, the ground state SAC calculation will be performed after the SAC-CI calculation in the excited state. Such a procedure is straightforward but it requires modifying the present framework of the SAC/SAC-CI implementation. In this paper we studied only vertical absorptions and adiabatic transitions, and the computations of routes 1–3 were implemented. The emission process in a solvent by PCM-SAC/SAC-CI will be addressed in a future study.

The single-point calculations were performed using the cc-pVDZ basis.[59] We also carried out the calculations using the larger basis, cc-pVTZ (Ref. 59) for C and O atoms and cc-pVDZ for H atoms. The equilibrium molecular geometries were optimized by the SAC and SAC-CI methods with the cc-pVDZ basis in equilibrium solvation. Furthermore, optimizations using the cc-pVTZ basis (for all atoms) were carried out in vacuum to compare the results with the previous studies. The perturbation-selection[60] was not used for the present calculations because the error resulting from the selection may compete with the solvent effects. We also performed the HF, second-order Møller–Plesset perturbation (MP2), and CIS calculations for the purpose of comparison. All the computations were performed with the GAUSSIAN development version and the direct SAC-CI program.[35] In SAC, SAC-CI, MP2, and CIS calculations the 1s electrons are excluded as frozen-core approximation. The present MP2 calculation with PCM is not self-consistent with the MP2 density, as implemented in Ref. 58; the PCM solvation effects are only taken into account through the HF MOs. This HF solvation will be a good approximation for the systems where electron correlations are not significant for the electron distributions, such as most organic molecules in their equilibrium geometry. The LR approach was used for the CIS calculations in which the transition density is used for

TABLE II. Ground state geometrical parameters (in angstroms and degrees) of s-*trans*-acrolein in vacuum.

	This work				Other works					Expt.	
	HF[a]	MP2[a]	SAC(DZ)[a]	SAC(TZ)[b]	CCSD[c]	CCSD(T)[c]	B3LYP[c]	CASPT2[d]	CASPT2[e]	Reference 63	Reference 64
O1C1	1.187	1.222	1.214	1.206	1.209	1.217	1.209	1.222	1.204	1.219	1.215
C1C2	1.480	1.483	1.491	1.479	1.477	1.477	1.471	1.467	1.473	1.470	1.468
C2C3	1.325	1.351	1.348	1.334	1.335	1.342	1.331	1.344	1.340	1.345	1.341
C1H1	1.104	1.122	1.121	1.105	1.105	1.108	1.109			1.108	1.113
C2H2	1.083	1.096	1.097	1.082	1.082	1.084	1.083			1.084	1.084
C3H3	1.082	1.094	1.096	1.080	1.081	1.083	1.081			1.086	1.081
C3H4	1.085	1.097	1.098	1.083	1.084	1.086	1.084			1.086	1.089
O1C1C2	123.9	124.2	124.0	124.2	124.1	124.1	124.4	124.2		123.2	123.9
O1C1H1	121.1	121.6	121.5	121.1	120.9	121.0	120.8			121.8	121.4
C1C2C3	121.3	120.5	120.9	120.6	120.5	120.3	121.1	120.5		119.5	120.3
C1C2H2	116.4	117.1	116.7	116.8	116.8	117.0	116.6			118.0	117.3
C2C3H3	122.0	122.0	122.0	122.1	122.1	122.1	122.2			121.3	122.2
C2C3H4	121.3	120.5	120.9	120.7	120.7	120.5	120.9			119.6	119.8

[a]cc-pVDZ basis set was used.
[b]cc-pVTZ basis set was used.
[c]Reference 44, aug-cc-pVTZ basis.
[d]Reference 41.
[e]Reference 43.

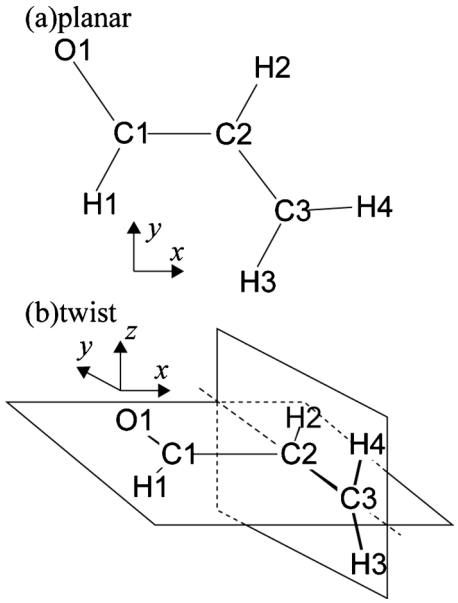

FIG. 2. Molecular structure and coordinate of acrolein (a) in planar conformation and (b) in twisted conformation.

the solvation in excited states; this is the default route in the PCM-CIS in the GAUSSIAN 09. The integral equation formalism PCM,[61] which is the default and recommended method, is used with the other default parameters of GAUSSIAN 09.[62]

B. s-*trans*-acrolein

Acrolein (C_3H_4O) is the simplest unsaturated aldehyde. It has conjugating double bonds and lone-pair electrons, and therefore it has low-lying $\pi \rightarrow \pi^*$ and $n \rightarrow \pi^*$ excited states. These features are of interest to spectroscopic and theoretical. UV spectra and the solvent effect have been studied using several methods and models.[40–45] Therefore, acrolein is a good example for the first application of the PCM-SAC-CI method.

Table II shows the optimized molecular geometries in the ground state in vacuum. The molecule is planar and the definitions of atomic labels are given in Fig. 2(a): the molecule was set in the x-y plane where the C1C2 bond was set to the x-axis. First we will discuss the molecular geometry in vacuum because its fundamental characteristics clarify solvent effects. The electron correlation increased the bond lengths, particularly for the double bonds C2C3 and O1C1. The SAC and MP2 showed a similar tendency, although the MP2 overestimated the correlation effects. In comparison with the experimental values, the MP2 result seems to be better than that of SAC with the cc-pVDZ basis. Shorter bond lengths were obtained when using the cc-pVTZ basis. The SAC/cc-pVTZ optimized geometry was almost identical to the geometry optimized with the CCSD/aug-cc-pVTZ, as reported in Ref. 44. Compared with experimental findings and other theoretical values, the accuracy of the SAC results is considered reasonable.

Table III shows the optimized molecular geometries in the lowest $n \rightarrow \pi^*(1\ ^1A'')$ and $\pi \rightarrow \pi^*(1\ ^1A')$ states. The $n \rightarrow \pi^*$ state has energy minimum in planar conformation, which was confirmed by the CIS calculation of the vibrational frequencies. For a start, the geometry of the $\pi \rightarrow \pi^*$ state was optimized with restrictions in the planar conformation. By the CIS calculation, the optimal planar structure has a negative frequency in the out-of-molecular-plane direction; therefore, it is not an energy minimum. A structure twisted around the C2C3 double bond has a lower energy than the planar conformation. This is an expected analogy with the lowest $\pi \rightarrow \pi^*$ state of ethylene. A minimum energy structure was then searched for around the structure twisted by 90° with restriction in the C_s point group. Two hydrogen atoms bonded to C3 were located out of the molecular plane and other atoms were placed on the molecular plane. The structure is shown in Fig. 2(b) and the optimized parameters are shown in Table III. This optimized structure ($1\ ^1A''$ state in

TABLE III. Geometrical parameters (in angstroms and degrees) of s-*trans*-acrolein in low-lying excited states in vacuum.

	$n \rightarrow \pi^*$ state						$\pi \rightarrow \pi^*$ state			
	This work			Other works		Expt.	Planar (this work)		Twisted (this work)	
	CIS[a]	SAC-CI[a]	SAC-CI[b]	CASPT2[c]	CASPT2[d]	Reference 65	CIS[a]	SAC-CI[a]	CIS[a]	SAC-CI[a]
O1C1	1.255	1.327	1.317	1.354	1.342	1.32	1.217	1.266	1.193	1.225
C1C2	1.454	1.422	1.411	1.371	1.381	1.35	1.431	1.455	1.470	1.462
C2C3	1.333	1.376	1.361	1.398	1.393	1.46	1.477	1.445	1.404	1.465
C1H1	1.095	1.107	1.092				1.109	1.125	1.100	1.119
C2H2	1.083	1.097	1.082				1.083	1.099	1.090	1.101
C3H3	1.081	1.094	1.079				1.081	1.095	1.087	1.102
C3H4	1.083	1.097	1.081				1.084	1.099	1.087	1.102
O1C1C2	123.7	124.8	124.4		124.4	125	123.7	122.3	123.2	123.1
O1C1H1	115.8	113.5	113.7				121.2	123.0	121.1	121.3
C1C2C3	124.7	123.5	123.5		123.4	125	123.7	125.2	124.7	123.3
C1C2H2	114.6	116.4	116.4				118.3	116.4	113.6	115.9
C2C3H3	120.1	120.6	120.6				120.1	121.2	122.6	121.5
C2C3H4	122.4	121.6	121.6				119.8	119.6	122.6	121.5
C1C2C3H4	180.0	180.0	180.0	180.0	180.0	180.0	180.0	180.0	92.8	93.2

[a]cc-pVDZ basis set was used.
[b]cc-pVTZ basis set was used.
[c]Reference 43.
[d]Reference 41.

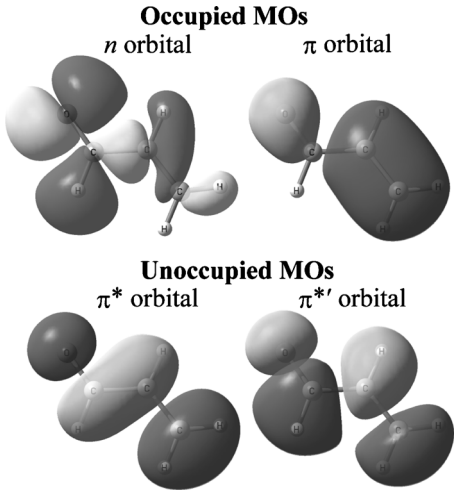

FIG. 3. Selected MOs of acrolein. The molecular plane is a nodal plane of π orbitals.

this coordinate) has no negative frequencies by the CIS calculation. If we remove the symmetry restriction in the C_s point group then the calculations become quite complex because intersections of potential surfaces may occur.[66] That subject is of importance in theoretical chemistry for excited states but it is beyond the scope of the present study. Therefore, we have studied excited state geometries and corresponding adiabatic excitations within a certain symmetry restriction.

Compared with ground state geometry, the lowest $n \rightarrow \pi^*$ excitation increases the O1C1 length and decreases the C1C2 length. This change in bond lengths reflects the character of the π^* orbital, which has antibonding character for O1C1 and C2C3 and bonding character for C1C2. The similar trend of geometry change upon the $n \rightarrow \pi^*$ excitation can be predicted qualitatively by the HF/CIS calculations, but the CIS calculation underestimates the effect of electronic excitation on molecular geometry. Results of microwave experiments propose bond alternation due to the excitation.[65] The experimentally proposed bond length seems to overestimate the bond alternation. The CASPT2 calculations have indicated slightly bond-alternated geometry for this state,[41,43] while the SAC-CI calculations could not reproduce the bond alternation. By analyzing the SAC-CI wave function, we found this state to have a multireference character that cannot be accurately described by the SAC-CI singles and doubles of R operators (SD-R) method. The main configurations in this state are $n \rightarrow \pi^*$ (0.9), $n \rightarrow \pi^{*\prime}$ (0.3), and $(n \rightarrow \pi^*)+(\pi \rightarrow \pi^*)$ (0.2), where the SAC-CI coefficient is in parentheses. We note $\pi^{*\prime}$ orbital as the next unoccupied π orbital whose orbital energy is higher than lowest unoccupied molecular orbital (LUMO). The isosurfaces of these orbitals are shown in Fig. 3. The last configuration denotes the double-excitation from the valence n and π orbital [highest occupied molecular orbital (HOMO) and next-HOMO] to the π^* orbital (LUMO); therefore the π^* orbital is doubly occupied in this configuration. Because of the importance of this configuration, the present SD-R calculation cannot accurately describe the geometry of this state.

Under the restriction on planar conformation, the $\pi \rightarrow \pi^*$ excitation increases the C2C3 and O1C1 lengths and decreases the C1C2 length; in particular, elongation of the C2C3 bond is significant. This can be explained by the electronic excitation from binding π to antibinding π^* orbital; consequently, the C2C3 bond becomes a single bond in the $\pi \rightarrow \pi^*$ state. While the HF/CIS calculations can describe such characteristics of electronic excitation, those calculations have overestimated the effect of electronic excitation.

For the twisted conformation of the $\pi \rightarrow \pi^*$ state, the O1C1 length decreases and the C2C3 length increases as compared to the planar conformation. Because of rotation around the C2C3 bond, that orbital is not purely a π^* orbital. It has an antibonding character for the C2C3 bond but has a

TABLE IV. Solvent effect on geometrical parameters ($pm=10^{-2}$ Å and degrees) of s-*trans*-acrolein with cc-pVDZ basis. Shifts from the vacuum value $[R(\text{in solv})-R(\text{in vac})]$ are shown.

	Ground state						$n \rightarrow \pi^*$				$\pi \rightarrow \pi^*$ (planar)				$\pi \rightarrow \pi^*$ (twisted)			
	SAC		MP2		HF		SAC-CI		CIS		SAC-CI		CIS		SAC-CI		CIS	
	hex.[a]	aq.[b]	hex.	aq.	hex.	aq.	hex.	aq.	hex.	aq.	hex.	aq.	hex.	aq.	hex.	aq.	hex.	aq.
O1C1	0.1	0.3	0.0	0.3	0.3	0.8	0.1	0.3	−0.2	−0.8	0.4	1.5	0.8	1.9	0.1	0.5	0.1	0.4
C1C2	−0.1	−0.3	−0.1	−0.4	−0.2	−0.5	−0.2	−0.7	0.5	1.5	1.3	4.4	−0.8	−1.8	−0.3	−0.9	0.3	0.8
C2C3	0.0	0.1	0.0	0.0	0.0	0.1	0.3	0.8	0.0	−0.2	−0.5	−1.9	0.4	1.1	0.2	0.6	−0.7	−1.9
C1H1	0.0	−0.2	−0.1	−0.3	−0.1	−0.3	0.0	0.0	0.2	0.5	−0.4	−1.1	−0.5	−1.2	−0.1	−0.2	−0.1	−0.2
C2H2	0.0	0.0	0.0	0.0	0.0	0.0	0.0	0.0	0.0	0.0	0.0	0.1	0.0	0.0	0.0	0.1	0.2	0.5
C3H3	0.0	0.0	0.0	0.0	0.0	0.0	0.0	0.0	0.0	0.1	0.0	0.1	0.0	0.1	0.0	0.2	0.1	0.2
C3H4	0.0	0.0	0.0	−0.1	−0.1	−0.1	0.0	0.0	0.0	0.0	0.0	0.0	−0.1	−0.1	0.0	0.2	0.1	0.2
O1C1C2	0.0	0.0	0.0	0.0	0.0	0.0	0.0	0.0	−0.1	0.1	−1.1	−2.9	−0.3	−0.7	0.3	0.6	0.0	0.0
O1C1H1	−0.1	−0.2	0.0	−0.2	−0.1	−0.3	0.0	−0.2	0.3	0.8	0.5	1.5	−0.5	−1.0	−0.1	−0.4	0.1	0.1
C1C2C3	−0.1	−0.3	−0.1	−0.3	−0.2	−0.5	−0.1	−0.4	−0.1	−0.2	1.0	2.1	0.9	1.5	−0.8	−2.1	−0.1	−0.2
C1C2H2	0.0	0.3	0.1	0.4	0.1	0.5	0.1	0.3	−0.1	−0.3	−0.5	−1.4	−0.4	−0.5	0.3	1.1	−0.4	−0.9
C2C3H3	0.0	−0.1	0.0	−0.1	−0.1	−0.2	0.0	0.0	−0.1	−0.3	−0.1	−0.4	−0.2	−0.5	−0.3	−1.5	0.1	0.4
C2C3H4	0.0	0.0	0.0	0.0	0.0	0.1	−0.1	−0.3	0.0	0.1	0.3	0.8	0.6	1.0	−0.3	−1.5	0.1	0.4
C1C2C3H4	0.0	0.0	0.0	0.0	0.0	0.0	0.0	0.0	0.0	0.0	0.0	0.0	0.0	0.0	1.8	7.5	−0.1	−0.3

[a]In *n*-hexane.
[b]In water.

slightly σ-bonding character for OC1. This orbital character consistently explains the changes of bond lengths in the twist conformation.

The solvent effects on the optimized geometry are given in Table IV, where we show the differences of the geometrical parameters between in solvent and in vacuum as

$$\Delta R(\text{solvent}) = R(\text{in solvent}) - R(\text{in vacuum}), \tag{94}$$

where R denotes a geometrical parameter. We chose water and n-hexane as typical polar and nonpolar solvents. The solvent effect on the equilibrium geometry of the ground state was small. A polar solvent increases the O1C1 length and decreases the C1C2 length. This trend can be described at the HF level but the solvent effect was overestimated without electron correlation. The solvent effect on the ground state equilibrium geometry calculated with the SAC method is similar to that of the MP2 calculations. This indicates that the coupling between the solvent effect and electron correlation is small because such a coupling effect is not considered by the present MP2 calculations. From the SAC calculations, the effects of polar and nonpolar solvents are similar. The effect of water is twofold or threefold of that of n-hexane.

To analyze the solvent effect on the excited state geometry, we focused on the geometry change due to excitation, i.e., the difference between the SAC and SAC-CI geometries optimized in each solvent. A geometrical parameter in an excited state R_e can be defined by the corresponding ground state parameter R_g and its change upon excitation ΔR_e as

$$R_e(\text{in vacuum/solvent}) = R_g(\text{in vacuum/solvent}) + \Delta R_e(\text{in vacuum/solvent}). \tag{95}$$

These parameters were defined both in vacuum and in solvent. Using Eqs. (94) and (95), we define the solvent effect on the geometry changes upon excitations as

$$\Delta\Delta R_e(\text{solvent}) = \Delta R_e(\text{in solvent}) - \Delta R_e(\text{in vacuum}), \tag{96}$$

which can be obtained from Table IV. The values of $\Delta\Delta R_e$ (water) for bond lengths are shown in Fig. 4, where the SAC/SAC-CI and the HF/CIS results are given by solid and broken lines, respectively. The solvent effect on ΔR_e is remarkably different between the SAC-CI and CIS calculations. The CIS calculation could not reproduce the SAC-CI results even qualitatively. For example, in the planar $\pi\rightarrow\pi^*$ state, according to the SAC-CI calculation, the C1C2 length increases in water, whereas the corresponding CIS calculation shows a decrease in the length. Such a significant failure could be ascribed to the LR approximation used in the present CIS calculation that cannot properly describe equilibrium solvation in excited states. The problem of LR approximation has been already shown.[21,24,25] TDDFT calculations may involve severe errors regarding the solvent effect on excited state geometries because, practically, LR approximation is used to evaluate solute-solvent interaction.

For the $n\rightarrow\pi^*$ excitation, values of ΔR_e are little affected by solvent. The solid lines in Fig. 4 of the $n\rightarrow\pi^*$ state are located within ± 1 pm. This means that the coupling effect between the electronic excitation and solvation on the molecular geometry is small for this state. The solvent effect on ΔR_e of the $\pi\rightarrow\pi^*$ state in planar conformation is larger than that of the $n\rightarrow\pi^*$ state. The solvent effect of water was 4.7 pm for the C1C2 bond. The solvent effect on ΔR_e of the twisted $\pi\rightarrow\pi^*$ state is also as small as that of the $n\rightarrow\pi^*$ state. The mechanism of the solvent effect will be analyzed later from the viewpoint of the electronic dipole moment.

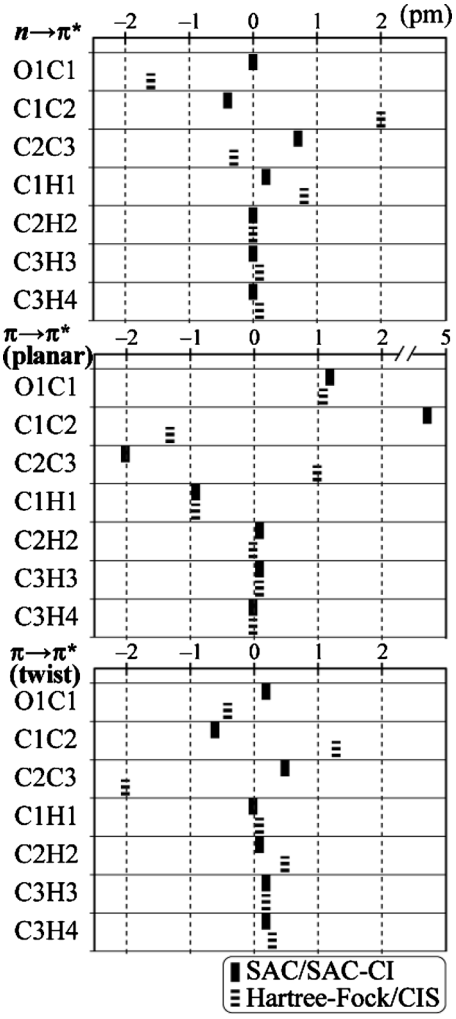

FIG. 4. Solvent effect on the changes of bond lengths (in picometers) upon electronic excitations for s-*trans*-acrolein. The solvent effect denotes the shift in aqueous solution from vacuum [defined by Eq. (96)].

Transition energies in vacuum are shown in Table V. The optimized geometries with the cc-pVDZ basis set were used for the present SAC/SAC-CI calculations and the cc-pVDZ and cc-pVTZ basis sets were used for the single-point calculations. The vertical excitation energy of the $n\rightarrow\pi^*$ state depends little on the basis sets. The SAC-CI results are similar to the CCSD/aug-cc-pVTZ results in Ref. 44 and they overestimated the experimental observations about 0.1–0.15 eV. As we mentioned earlier, this state has a considerable multireference contribution, and therefore, these single-reference single and double methods are poor. The importance of triples has been reported with the CC3 and CCSDR(3) calculations,[70] and this is consistent with findings that the agreement with experiment is better when using the CASPT2 calculations than when using the CCSD and

TABLE V. Excitation energies (in eV) of s-*trans*-acrolein in vacuum.

	Vertical		Adiabatic		
Method	$n \rightarrow \pi^*$	$\pi \rightarrow \pi^*$	$n \rightarrow \pi^*$	$\pi \rightarrow \pi^*$ (planar)	$\pi \rightarrow \pi^*$ (twisted)
SAC-CI (DZ)[a]	3.84	7.19	3.43	6.82	2.66
SAC-CI (TZ)[b]	3.85	6.97	3.51	6.68	2.74
CCSD[c]	3.89	6.84			
CC3[c]	3.75	6.65			
CCSD[d]	3.91	6.87			
CCSDR(3)[d]	3.81	6.73			
CAM-B3LYP[c]	3.80	6.40			
CASSCF[e]	3.93	7.54	3.19		
CASPT2[e]	3.63	6.94	3.12		
MSCASPT2[e]	3.63	6.10			
CASSCF[f]	3.97		3.16		
CASPT2[f]	3.77		3.10		
Expt.	3.75[g]	6.41[h]	3.21[i]		
	3.69[c]	6.42[c]			

[a]cc-pVDZ basis with cc-pVDZ geometry.
[b]cc-pVTZ basis with cc-pVDZ geometry.
[c]Reference 44.
[d]Reference 70.
[e]Reference 41.
[f]Reference 43.
[g]Reference 67.
[h]Reference 68.
[i]Reference 65.

SAC-CI calculations. The optimized geometry in the $n \rightarrow \pi^*$ state was inaccurate. Hence, the SAC-CI calculation significantly overestimated the adiabatic transition energy of the $n \rightarrow \pi^*$ state.

The vertical excitation energy of the $\pi \rightarrow \pi^*$ state significantly depends on the basis set. The SAC-CI and CCSD calculations still overestimated the experimental observations. The CC3 calculations showed the remarkable importance of triple excitations for this state.[44] Here we should note the definition of the vertical excitation energy of an experiment. In the experimental value, it was assumed that the vertical transitions correspond to the observed peak maxima but this is not always true. Molecular vibration and geometry relaxation could affect the experimental peak structure. Indeed, the adiabatic transition energies to the planar and twisted conformations were much lower than the

TABLE VI. Solvent shift from vacuum value for excitation energies (in eV) of s-*trans*-acrolein.

	Vertical				Adiabatic					
	$n \rightarrow \pi^*$		$\pi \rightarrow \pi^*$		$n \rightarrow \pi^*$		$\pi \rightarrow \pi^*$ (planar)		$\pi \rightarrow \pi^*$ (twisted)	
Method	hex.[a]	aq.[b]	hex.	aq.	hex.	aq.	hex.	aq.	hex.	aq.
SAC-CI (DZ)[c]	−0.01	+0.08	−0.15	−0.25	−0.01	−0.04	−0.09	−0.30	−0.04	−0.01
SAC-CI (TZ)[d]	−0.01	+0.10	−0.10	−0.22	−0.01	−0.03	−0.09	−0.32	−0.01	−0.01
CCSD[e]		+0.23		−0.41						
CCSD[f]		+0.25		−0.33						
CCSDR(3)[f]		+0.26		−0.35						
CAM-B3LYP[e]		+0.26		−0.47						
CASPT2[g]		+0.33		−0.10						
CASSCF[h]		+0.19				+0.14				
CASPT2[h]		+0.19				+0.12				
Experiment[i]		+0.2		−0.4						

[a]In *n*-hexane.
[b]In water.
[c]cc-pVDZ basis with cc-pVDZ geometry.
[d]cc-pVTZ basis with cc-pVDZ geometry.
[e]Reference 44, QM/MM.
[f]Reference 70, QM/MM with no water in QM.
[g]Reference 41, PCM.
[h]Reference 43, QM/MM.
[i]References 36–39.

TABLE VII. Dipole moment (debye) of s-*trans*-acrolein. The dipole moment |d| and its Cartesian components are shown.

	Vacuum				Aqueous			
State	x	y	z	|d|	x	y	z	|d|
Ground	1.961	1.938	0.000	2.757	2.508	2.341	0.000	3.431
$n\rightarrow\pi^*$	1.116	0.463	0.000	1.208	1.299	0.418	0.000	1.364
$\pi\rightarrow\pi^*$ (planar)	3.003	4.072	0.000	5.060	4.401	6.187	0.000	7.593
$\pi\rightarrow\pi^*$ (twisted)	1.917	2.075	0.000	2.825	2.235	2.667	0.000	3.480

vertical excitation energy calculated with the SAC-CI. This implies the significance of the relaxation and vibration effects.

The shifts of transition energies by solvent from the vacuum are shown in Table VI; the positive value denotes that excitation energy increases in solvent (blue shift). Polar solvent increases the vertical excitation energy of the $n\rightarrow\pi^*$ state because equilibrium solvation stabilized the ground state more than the excited state, in which nonequilibrium solvation was used. The shift in aqueous solution was 0.10 eV, as calculated with SAC-CI/cc-pVTZ. The calculated solvent shift was smaller than the experimental and other theoretical results. This underestimation could be attributed to the lack of hydrogen bonds from explicit solvent molecules and an insufficient description of charge separation in the excited state. The CCSD and QM/MM model with the CCSD method provided a larger solvent shift.[44] The effects of triple excitations by the CCSDR(3) are canceled in the solvent shift.[70] The CASPT2 calculation[41] that appropriately describes the excited state also provided a larger solvent shift even if only the PCM was used. The solvent effect decreases the adiabatic excitation energy; the shift in aqueous solution in the $n\rightarrow\pi^*$ state was -0.03 eV, calculated with the cc-pVTZ basis. The CASPT2 result[43] of this shift was 0.12 eV, and was significantly different from the SAC-CI result. This discrepancy was probably caused by the difference in the optimized geometry of the excited state.

The solvent shifts of the vertical $\pi\rightarrow\pi^*$ excitation were negative. The excited state is stabilized more than the ground state, even by nonequilibrium solvation. Such a remarkable solvent effect on the excited state can be explained by the dipole moment of molecule; the Cartesian components and the norm |d| are shown in Table VII for vacuum and an aqueous environment. The dipole moment of the $\pi\rightarrow\pi^*$ state in planar conformation is twice as large as that of the ground state. The polarized $\pi\rightarrow\pi^*$ state is stabilized by polar solvent more than the ground state is, and a redshift is observed. The solvent shift calculated with SAC-CI/PCM is small in comparison with the experimental findings. The CASPT2/PCM also underestimated the solvent shift.[41] The CCSDR(3) calculation showed that the effect of triple excitations on the solvent shift is minor.[70] The importance of the QM treatment of water molecules was reported in Ref. 44. The solvent shift of the vertical $\pi\rightarrow\pi^*$ excitation energy strongly depends on the number of QM water. We also note that the observed peak of the $\pi\rightarrow\pi^*$ transition is broad and vibration and other effects for spectral shape must be considered to predict the accurate solvatochromic effect on spectroscopy. These points have been discussed in the recent QM/MM study by Sneskov *et al.*[70]

The solvent shift in water becomes large in the adiabatic $\pi\rightarrow\pi^*$ excitation of the planar conformation in comparison with the vertical excitation because the equilibrium solvation further stabilizes the polarized $\pi\rightarrow\pi^*$ state. The geometry relaxation distorting planar conformation causes reorganization of electron distribution of this state. The dipole moment of the twisted $\pi\rightarrow\pi^*$ state is similar to that of the ground state. The absolute solvent effect on the ground and the twisted $\pi\rightarrow\pi^*$ states are canceled out, and thus the solvent shift of the adiabatic transition energies to the twisted $\pi\rightarrow\pi^*$ state becomes very small.

The Mulliken atomic charges are shown in Table VIII.

TABLE VIII. Mulliken atomic charges of s-*trans*-acrolein computed with the SAC/SAC-CI effective density matrix.

	Vacuum				Aqueous			
	Ground	$n\rightarrow\pi^*$	$\pi\rightarrow\pi^*$ (planar)	$\pi\rightarrow\pi^*$ (twisted)	Ground	$n\rightarrow\pi^*$	$\pi\rightarrow\pi^*$ (planar)	$\pi\rightarrow\pi^*$ (twisted)
O1	−0.208	−0.146	−0.358	−0.211	−0.257	−0.163	−0.456	−0.262
C1	0.200	0.118	0.175	0.184	0.209	0.121	0.099	0.190
H1	0.002	0.071	−0.016	−0.001	0.024	0.096	−0.010	0.018
C2	−0.149	−0.130	−0.090	−0.120	−0.161	−0.149	−0.059	−0.111
H2	0.043	0.039	0.067	0.057	0.047	0.048	0.081	0.065
C3	−0.002	−0.039	0.066	−0.070	−0.003	−0.061	0.125	−0.077
H3	0.052	0.036	0.074	0.080	0.067	0.049	0.105	0.089
H4	0.062	0.050	0.083	0.080	0.074	0.058	0.114	0.089
Formyl[a]	−0.006	0.043	−0.200	−0.028	−0.024	0.054	−0.367	−0.054
Vinyl[b]	0.006	−0.044	0.200	0.028	0.024	−0.054	0.367	0.054

[a]Total atomic charges of formyl group (O1C1H1).
[b]Total atomic charges of vinyl group (C2H2C3H3H4).

TABLE IX. Geometrical parameters (angstroms and degrees) of methylenecyclopropene in vacuum.

	Ground state						$\pi \rightarrow \pi^*$ (planar)		$\pi \rightarrow \pi^*$ (twist)	
	HF[a]	MP2[a]	SAC(DZ)[a]	SAC(TZ)[b]	CASSCF[c]	Expt.[d]	SAC-CI[a]	CIS[a]	SAC-CI[a]	CIS[a]
C1C2	1.433	1.460	1.463	1.443	1.443	1.441	1.372	1.357	1.496	1.470
C2C3	1.309	1.343	1.337	1.319	1.323	1.323	1.510	1.486	1.326	1.298
C1C4	1.325	1.342	1.341	1.328	1.336	1.332	1.464	1.398	1.445	1.396
C2H1	1.076	1.090	1.091	1.076	1.073	1.080	1.084	1.070	1.091	1.076
C4H3	1.076	1.090	1.091	1.076	1.073	1.080	1.094	1.078	1.095	1.081
C4H4	1.081	1.092	1.094	1.080	1.080	1.085	1.094	1.078	1.103	1.093
C2C1C3	54.4	54.7	54.4	54.4			66.8	66.4	52.6	52.4
C1C2H1	149.0	149.6	149.1	149.1		147.5	151.1	151.4	147.7	146.6
C1C4H3	120.7	120.5	120.7	120.7		121	120.1	120.4	121.0	121.8
C1C4H4	120.7	120.5	120.7	120.7		121	120.1	120.4	120.1	121.8
oop[e]									38.3	35.7

[a]cc-pVDZ basis set was used.
[b]cc-pVTZ basis set was used.
[c]Reference 48.
[d]Reference 69.
[e]Out-of-plane angle, see Fig. 5.

The gross charge of formyl (OCH) and vinyl ($CHCH_2$) groups are shown. Notable charge separation is observed for the planar $\pi \rightarrow \pi^*$ state in which the gross charge of the formyl group is -0.200. The charge of the formyl group in the ground state is -0.006; therefore, this state has an intramolecular electron transfer character from vinyl to formyl in 0.194. This electron transfer character enlarges the dipole moment of this state, and consequently enhances the solvent effect in polar solvent.

The charge separation in the $n \rightarrow \pi^*$ state is slightly larger than that in the ground state and the direction is different from that of the ground state. The formyl group is positive in the $n \rightarrow \pi^*$ state, whereas it has small negative charge in the ground state. Therefore, the equilibrium orientations of polar solvent are different between the ground state and the $n \rightarrow \pi^*$ state. The nonequilibrium solvation does not stabilize the $n \rightarrow \pi^*$ state and it causes a blueshift of vertical excitation energy. The equilibrium solvation stabilizes the charge separated $n \rightarrow \pi^*$ state well, and this effect reduces the adiabatic transition energy. The charge distribution of the twisted $\pi \rightarrow \pi^*$ state is similar to that of the ground state, thus solvent shift by the polar solvent is very small because the absolute effects are cancelled out in the ground and excited states.

C. Methylenecyclopropene

The excited state properties of methylenecyclopropene (C_4H_4) and their solvent dependence are interesting because of methylenecyclopropene's sudden polarization effect: The dipole moments in the ground and the first excited state are opposite. These properties have been studied using several different methods.[16,46,48,49] It is possible to drastically change molecular properties by light absorption.

Table IX shows the optimized molecular geometries in the ground state and the lowest $\pi \rightarrow \pi^*$ excites state in vacuum. The ground state is planar. Definitions of the atomic labels are given in Fig. 5(a): the molecule with C_{2v} point group symmetry was placed in the y-z plane where the principal axis is in the z-direction. The geometry in the lowest $\pi \rightarrow \pi^*$ state ($1\ ^1B_2$) was first optimized within planar conformation. The optimal structure is shown in Table IX. With this restricted geometry, two negative frequencies are obtained in the direction of out-of-plane motion by the CIS calculation. Therefore, this planar structure is not an energy minimum. A minimum energy structure was searched within 90° twisted conformation. We found a twisted and bent structure, as shown in Fig. 5(b), in which negative frequencies were not obtained by the CIS calculation. Here, we still used a symmetry restriction in the C_s point group during geometry optimization. We suppose that a structure of lower energy would exist without symmetry restriction. In the present

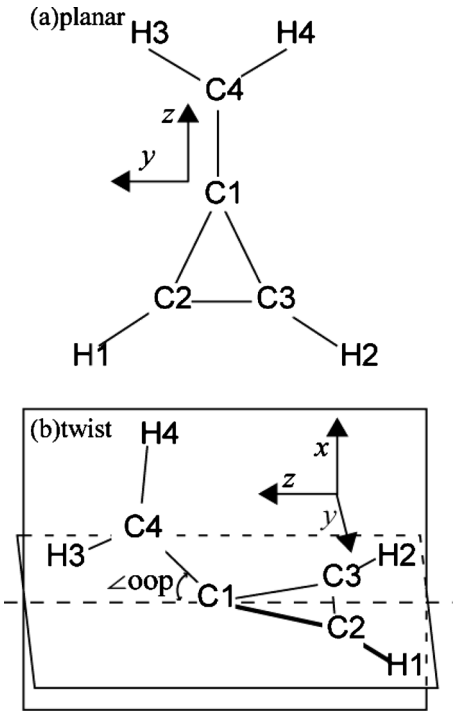

FIG. 5. Molecular structure and coordinate of methylenecyclopropene (a) in planar conformation and (b) in twisted conformation.

TABLE X. Solvent effect on geometrical parameters (pm=10^{-2} Å and degrees) of methylenecyclopropene with cc-pVDZ basis. Shifts from the vacuum value [R(in solv)−R(in vac)] are shown.

	Ground state						$\pi\rightarrow\pi^*$ (planar)				$\pi\rightarrow\pi^*$ (twisted)			
	SAC		MP2		HF		SAC-CI		CIS		SAC-CI		CIS	
	hex.[a]	aq.[b]	hex.	aq.	hex.	aq.	hex.	aq.	hex.	aq.	hex.	aq.	hex.	aq.
C1C2	−0.2	−0.3	0.0	−0.2	−0.2	−0.5	0.1	0.3	0.7	2.5	0.0	0.2	0.4	1.2
C2C3	0.0	0.1	0.0	0.1	0.1	0.2	0.4	1.2	0.3	0.9	0.0	0.1	−0.1	−0.3
C1C4	0.1	0.3	0.1	0.3	0.2	0.6	0.2	0.4	−1.1	−3.4	−0.1	−0.3	−0.6	−1.7
C2H1	0.0	0.0	0.0	0.0	0.0	0.0	0.0	0.0	0.0	0.2	0.1	0.1	0.1	0.1
C4H3	0.0	0.0	0.0	0.0	0.0	0.0	0.0	0.1	0.1	0.1	−0.1	−0.1	0.1	0.3
C4H4	0.0	0.1	0.1	0.1	0.0	0.1	0.0	0.1	0.1	0.1	0.1	0.1	0.2	0.5
C2C1C3	0.1	0.1	0.1	0.2	0.1	0.2	0.1	0.4	−0.3	−0.9	0.0	0.0	−0.2	−0.6
C1C2H1	0.0	0.0	−0.3	−0.3	−0.1	−0.1	0.0	0.7	0.1	0.1	−0.3	−0.6	−0.3	−0.9
C1C4H3	0.0	0.0	−0.3	−0.3	−0.1	−0.1	−0.2	−0.2	0.1	0.2	0.4	1.0	0.3	0.7
C1C4H4	0.0	0.0	0.0	0.1	0.0	0.0	−0.2	−0.2	0.0	0.2	0.6	0.0	0.0	0.1
oop[c]											−0.5	−1.3	−0.2	−1.1

[a]In n-hexane.
[b]In water.
[c]Out-of-plane angle, see Fig. 5.

study, however, we do not discuss such a possibility because it is beyond the scope of our purpose, although it is important to explore the potential energy surface for understanding photochemistry.

In the ground state, electron correlation increases the bond lengths. The optimized molecular structures with the SAC and MP2 are almost identical. Using a larger basis set reduces the bond lengths, and the SAC/cc-pVTZ calculation reproduces the experimental structure with good accuracy. In the planar conformation, the $\pi\rightarrow\pi^*$ excitation changes the position of the double bonds. In this state, the C2C3 and C1C4 lengths are significantly increased and the C1C2 length is decreased. The HF/CIS calculation could reproduce the trend as calculated by the SAC/SAC-CI. In the twisted conformation, the bond lengths are similar to those of the ground state rather than the planar $\pi\rightarrow\pi^*$ state. The electronic wave function in the $\pi\rightarrow\pi^*$ state is relaxed according to the geometrical relaxation. The HF/CIS calculations well reproduce the change in geometry upon the electronic excitation calculated by the SAC/SAC-CI because this molecule (methylenecyclopropene) has less geometrical freedom than acrolein.

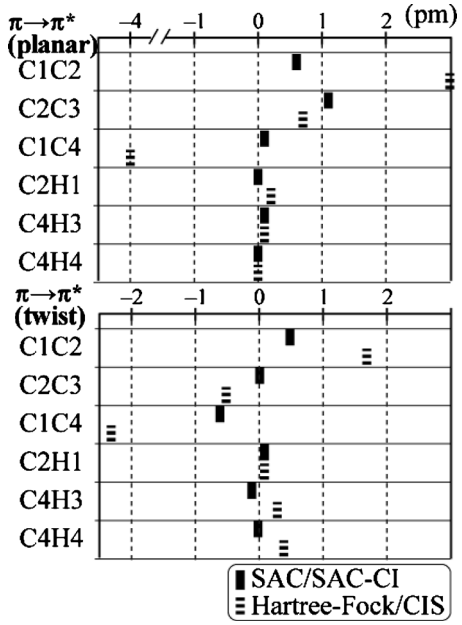

FIG. 6. Solvent effect on the changes of bond lengths (in picometers) upon electronic excitations for methylenecyclopropene. The solvent effect denotes the shift in aqueous solution from vacuum [defined by Eq. (96)].

The solvent effects on the optimized geometry in n-hexane and aqueous solution are shown in Table X, in which the differences of geometrical parameters are given as defined by Eq. (94). The solvent effects are negligible for the ground state geometry because the molecule is highly symmetric and has a rigid ring structure. The HF calculation tends to overestimate the solvent effect, although it is still very small.

The values of $\Delta\Delta R_e$ defined by Eq. (96) for the $\pi\rightarrow\pi^*$ state in aqueous solution are shown in Fig. 6, where the SAC/SAC-CI and the HF results are given by solid and bro-

TABLE XI. Excitation energies (in eV) of methylenecyclopropene in vacuum.

Method	Vertical	Adiabatic (planar)	Adiabatic (twisted)
SAC-CI(DZ)[a]	4.73	3.53	2.77
SAC-CI(TZ)[b]	4.76	3.57	2.88
CASSCF (DZ)[c]	4.63		
CASSCF (TZ)[c]	4.56		
CASSCF[d]	4.71		
CASPT2[d]	4.13		
Expt.[e]	4.01 (n-pentane)[f]		
	4.49 (MeOH)[g]		

[a]cc-pVDZ basis with cc-pVDZ geometry.
[b]cc-pVTZ basis with cc-pVDZ geometry.
[c]Reference 48.
[d]Reference 49.
[e]Reference 47.
[f]In n-pentane −78 °C.
[g]In methanol −78 °C.

TABLE XII. Solvent shift on excitation energies (in eV) of methylenecyclopropene.

	Vertical			Adiabatic (planar)		Adiabatic (twisted)	
Method	Nonpolar[a]	Polar[b]	Shift[c]	Nonpolar	Polar	Nonpolar	Polar
SAC-CI (DZ)[d]	−0.06	+0.11	0.17	−0.04	−0.11	0.00	0.00
SAC-CI (TZ)[e]	−0.07	+0.13	0.20	−0.05	−0.11	0.00	0.00
CASPT2 (DZ)[f]	−0.01	+0.16	0.17				
CASPT2 (TZ)[f]	−0.01	+0.18	0.19				
Expt.[g]			0.48				

[a]In nonpolar solvent, *n*-hexane for SAC-CI.
[b]In polar solvent, water for SAC-CI.
[c]Nonpolar to polar solvent shift, *n*-pentane to methanol for experiment.
[d]cc-pVDZ basis with cc-pVDZ geometry.
[e]cc-pVTZ basis with cc-pVDZ geometry.
[f]Reference 48, PCM.
[g]Reference 47.

ken lines, respectively. The LR approximated CIS calculation cannot provide a reliable prediction of the solvent effect even in its qualitative trend. The solvent effect on ΔR_e is very small; it is less than 1 pm. The solvent effect on the geometrical parameters is quite small for methylenecyclopropene while the effect on the excitation energy is significant.

Table XI shows the excitation energies in vacuum. The basis set dependence of the excitation energy is not very large. The SAC-CI calculation overestimated the vertical excitation energy by about 0.6 eV, compared with the case of the experiment in *n*-pentane. Except for experimental uncertainty, because of peak broadness, this discrepancy could be attributed to the lack of triple and higher excitations. The maximum coefficient of double excitations in the present SAC-CI calculation was 0.3, and therefore the state has a weak multielectron excitation character. The present singles and doubles SAC-CI calculation is less adequate for very accurate calculations. The CASPT2 study[49] yielded better excitation energy than was obtained using the SAC-CI method. The geometrical relaxation in an excited state remarkably affects the transition energy. Even in planar conformation, the adiabatic transition energy is 1.2 eV less than the vertical excitation energy owing to the bond alternation that occurs in the $\pi \rightarrow \pi^*$ state. The twist of the C1C4 bond further stabilizes the excited state. These relatively large relaxations cause the absorption peak to be broader.

The solvent shifts of transition energies from the vacuum are shown in Table XII. The polar and nonpolar solvents for the SAC-CI calculation were water and *n*-hexane, respectively. The polar solvent increases the vertical excitation energy but the nonpolar solvent decreases it. The direction of the dipole moment of methylenecyclopropene is changed by the excitation. The orientation of polar solvent to the ground state destabilizes the excited state because the direction of the dipole moment is opposite. In nonpolar solvent, stabilization by solvent in the ground state and the excited state are similar, and the effect results in a small redshift. The solvent effects on the adiabatic transitions become small even in a polar solvent because equilibrium solvation similarly affects the ground and excited states. The calculated nonpolar to polar solvent shift is 0.2 eV. This result is close to that of the CASPT2 calculation,[49] and significantly underestimates the experimental findings.[47] Explicit solvent molecules treated by a QM method may be important to reproduce the solvent shift by the analogy of the $\pi \rightarrow \pi^*$ transition of acrolein.

The calculated dipole moments, the Cartesian component, and the norm are shown in Table XIII. The moments in the ground and planar $\pi \rightarrow \pi^*$ states have opposite signs. The direction of the twisted $\pi \rightarrow \pi^*$ state is the same as the ground state. The atomic charges are shown in Table XIV. The charge separation between ring and methylene is induced by the $\pi \rightarrow \pi^*$ excitation in planar conformation. The twisted $\pi \rightarrow \pi^*$ state has rather small atomic charges. A zwitterionic character proposed by Johnson and Schmidt[46] was not obtained for the twisted conformation in the present calculation, probably because we have used bond lengths of twisted conformation optimized in the excited state. The relaxation of bond lengths significantly affects the atomic charge distribution in the excited state. The present calculations show the importance of the optimization of excited state geometry to study the sudden polarization effect of methylenecyclopropene and other related phenomena. The present PCM SAC-CI method has the potential for such applications.

V. CONCLUSIONS

In this paper we presented the theory, implementation, and applications of the SAC/SAC-CI method, including the solvent effect, by means of the PCM. The PCM-SAC/SAC-CI theory was developed to study the electronic excitation of molecules in solution. The PCM theory has been incorporated into the SAC and SAC-CI theories by considering an energy functional approach, which gives a consistent formulation, like the variational principle, although we used the nonvariational theory of the SAC and SAC-CI. The analytical energy gradient of the PCM-SAC and PCM-SAC-CI was formulated in terms of the SAC and SAC-CI energy functional. The PCM-SAC-CI method is a SS approach, in which the solute-solvent interaction operators depend on the QM charge distribution of the solute in the specific excited states.

TABLE XIII. Dipole moment (debye) of methylenecyclopropene. The dipole moment |d| and its Cartesian components are shown.

	Vacuum					Aqueous			
State	x	y	z	|d|	Expt.[a]	x	y	z	|d|
Ground	0.000	0.000	−1.859	1.859	1.90	0.000	0.000	−2.462	2.462
$\pi \rightarrow \pi^*$ (planar)	0.000	0.000	1.195	1.195		0.000	0.000	1.421	1.421
$\pi \rightarrow \pi^*$ (twisted)	0.334	0.000	−1.177	1.223		0.860	0.000	−1.158	1.442

[a]Reference 69.

The PCM-SAC and PCM-SAC-CI theories were implemented on the latest version of the SAC-CI program incorporated with the GAUSSIAN development version. It is possible to perform the molecular geometry optimization in solution in the ground and excited states. Several combinations of molecular geometry, the target electronic state, and solvation models (equilibrium or nonequilibrium) are available. Some typical calculation routes are presented, for example, solvatochromism of electronic spectra, adiabatic transitions, and photochemical reactions in solution.

The equilibrium geometry and electronic transitions of s-*trans*-acrolein and methylenecyclopropene were studied with the PCM-SAC and PCM-SAC-CI methods in vacuum and in nonpolar and polar solvents. The SAC calculations could well reproduce the experimental geometry in vacuum. It is possible to calculate the energy, wave function, and optimized geometry using the PCM-SAC method, in which both the electron correlation and solvent effects are self-consistently taken into account. For the ground state geometry of these molecules, the coupling of the electron correlation and solvent effects was small.

The PCM-SAC-CI method can calculate the energy, wave function, and optimized geometry in solution by considering the electron correlation with the SS approach. The effect of solvents on the vertical and adiabatic excitation energies were studied for s-*trans*-acrolein. The effects on the lowest $n \rightarrow \pi^*$ and $\pi \rightarrow \pi^*$ states of s-*trans*-acrolein are red- and blueshifts, respectively, for the vertical excitations. The PCM-SAC/SAC-CI can reproduce the observed trends but the shifts were underestimated, probably because of the lack of explicit solvent molecules. The excited state geometry was optimized in vacuum and in solution. The nonplanar twisted geometry was found in the $\pi \rightarrow \pi^*$ state. The solvent effects on the ground and excited states were investigated with the dipole moment and Mulliken charges. Relatively large charge polarization was obtained for the $\pi \rightarrow \pi^*$ state.

The redshift was obtained for the lowest vertical $\pi \rightarrow \pi^*$ excitation of methylenecyclopropene in polar solution. The observed trend was reproduced but the shift value was underestimated by the PCM-SAC/SAC-CI calculations. Adiabatic transition was studied and large geometry relaxation was obtained. The calculated dipole moment and Mulliken charges explained the mechanism of solvation in the ground and excited states.

The solvent effects on the optimized geometry in the excited state differ significantly between the PCM-SAC-CI and CIS results. This discrepancy could be attributed to the LR approximation used in the CIS calculation. The present study shows the importance of the SS approach to study the excited states; the LR approach may cause serious errors.

In this paper the PCM-SAC/SAC-CI equations are presented in the Hamiltonian matrix formula. The Hamiltonian matrix algorithm has been replaced by the MO integral direct algorithm in the latest SAC-CI program. The PCM-SAC/SAC-CI in the MO integral direct algorithm will be reported in a forthcoming paper. The presented formulation is applicable to other spin states. The implementation of triplet and doublet states is straightforward, and will also be reported in a forthcoming paper.

TABLE XIV. Mulliken atomic charges of methylenecyclopropene computed with the SAC/SAC-CI effective density matrix.

	Vacuum			Aqueous		
	Ground	$\pi \rightarrow \pi^*$ (planar)	$\pi \rightarrow \pi^*$ (twisted)	Ground	$\pi \rightarrow \pi^*$ (planar)	$\pi \rightarrow \pi^*$ (twisted)
C1	−0.003	0.075	−0.076	−0.015	0.081	−0.115
C2	−0.025	−0.124	−0.018	−0.021	−0.149	−0.023
C3	−0.025	−0.124	−0.018	−0.021	−0.149	−0.023
H1	0.046	0.035	0.045	0.069	0.050	0.066
H2	0.046	0.035	0.045	0.069	0.050	0.066
C4	−0.103	−0.040	−0.077	−0.149	−0.050	−0.086
H3	0.032	0.071	0.042	0.035	0.083	0.051
H4	0.032	0.071	0.057	0.035	0.083	0.064
Ring[a]	0.039	−0.103	−0.022	0.080	−0.117	−0.029
Me[b]	−0.039	0.103	0.022	−0.080	0.117	0.029

[a]Total atomic charges of ring (C1C2C3H1H2).
[b]Total atomic charges methylene group (C4H3H4).

ACKNOWLEDGMENTS

R.C. thanks the Italian MIUR "Ministero dell'Istruzione, Universitae Ricerca," for financial support (Grant No. PRIN2007). M.E. and R.F. acknowledge support from a Grant-in-Aid for Scientific Research from the Japan Society for the Promotion of Science, the Next Generation Supercomputing Project, and the Molecular-Based New Computational Science Program, NINS. The computations were partly performed using the Research Center for Computational Science, Okazaki, Japan.

APPENDIX: PCM-SAC EQUATIONS FOR THE Z-AMPLITUDES

The explicit form of the Z-amplitude equations for the PCM-SAC in Eq. (40) and its detailed derivation are presented here. The PCM SAC energy functional is given as

$$L_{\mathrm{PCM}}^{\mathrm{SAC}} = \sum_I C_I \bar{H}_{0I}^{\mathrm{HF}} \left(1 - \sum_K \sum_I Z_K C_I \bar{S}_{KI}\right) + \sum_K Z_K \left(H_{K0}^{\mathrm{HF}} + \sum_I C_I \bar{H}_{KI}^{\mathrm{HF}}\right) + \frac{1}{2}\Delta Q_{\mathrm{SAC}} \Delta V_{\mathrm{SAC}}, \tag{A1}$$

where

$$\Delta Q_{\mathrm{SAC}} = \sum_I C_I Q_{0I} \left(1 - \sum_K \sum_I Z_K C_I \bar{S}_{KI}\right) + \sum_K Z_K \left(Q_{K0} + \sum_I C_I \bar{Q}_{KI}\right) \tag{A2}$$

and

$$\Delta V_{\mathrm{SAC}} = \sum_I C_I V_{0I} \left(1 - \sum_K \sum_I Z_K C_I \bar{S}_{KI}\right) + \sum_K Z_K \left(Q_{K0} + \sum_I C_I \bar{V}_{KI}\right). \tag{A3}$$

The PCM-Z-SAC equations can be obtained as Eq. (40),

$$\frac{\partial L_{\mathrm{PCM}}^{\mathrm{SAC}}}{\partial C_I} = 0 = \bar{\bar{H}}_{0I}^{\mathrm{PCM}} + \sum_K Z_K Y_{KI}^{\mathrm{PCM}} + \sum_{KL} Z_K Z_L W_{KLI}. \tag{A4}$$

The differentiation of the energy functional may be written as follows:

$$\frac{\partial L_{\mathrm{PCM}}^{\mathrm{SAC}}}{\partial C_I} = \bar{\bar{H}}_{0I}^{\mathrm{HF}} - \bar{\bar{H}}_{0I}^{\mathrm{HF}} \sum_K \sum_J Z_K C_J \bar{S}_{KJ} - \sum_J C_J \bar{H}_{0J}^{\mathrm{HF}} \sum_K Z_K \bar{\bar{S}}_{KI} + \sum_K Z_K \bar{\bar{H}}_{KI}^{\mathrm{HF}} + \frac{1}{2}\frac{\partial \Delta Q_{\mathrm{SAC}}}{\partial C_I}\Delta V_{\mathrm{SAC}} + \frac{1}{2}\Delta Q_{\mathrm{SAC}}\frac{\partial \Delta V_{\mathrm{SAC}}}{\partial C_I}, \tag{A5}$$

where

$$\frac{\partial \Delta Q_{\mathrm{SAC}}}{\partial C_I} = Q_{0I} - Q_{0I}\left(\sum_K \sum_J Z_K C_J \bar{S}_{KJ}\right) - \sum_J C_J Q_{0J}\left(\sum_K Z_K \bar{\bar{S}}_{KI}\right) + \sum_K Z_K \bar{\bar{Q}}_{KI} \tag{A6}$$

and

$$\frac{\partial \Delta V_{\mathrm{SAC}}}{\partial C_I} = V_{0I} - V_{0I}\left(\sum_K \sum_J Z_K C_J \bar{S}_{KJ}\right) - \sum_J C_J V_{0J}\left(\sum_K Z_K \bar{\bar{S}}_{KI}\right) + \sum_K Z_K \bar{\bar{V}}_{KI}. \tag{A7}$$

The corresponding SAC energy in terms of the Hamiltonian with fixed HF field can be defined by

$$\Delta E_{\mathrm{SAC}}^{\mathrm{HF}} = \sum_J C_J \bar{H}_{0J}^{\mathrm{HF}}. \tag{A8}$$

For a clear expression we define similar notations in terms of Q and V by

$$\sum_J C_J Q_{0J} = \Theta_{\mathrm{SAC}} \tag{A9}$$

and

$$\sum_J C_J V_{0J} = \mathrm{s}_{\mathrm{SAC}}. \tag{A10}$$

Inserting Eqs. (A2), (A3), and (A6)–(A10) into Eq. (A5), we obtain

$$\frac{\partial L_{\mathrm{PCM}}^{\mathrm{SAC}}}{\partial C_I} = \bar{\bar{H}}_{0I}^{\mathrm{HF}} + \sum_K Z_K \left(\bar{\bar{H}}_{KI}^{\mathrm{HF}} - \bar{\bar{H}}_{0I}^{\mathrm{HF}} \sum_J C_J \bar{S}_{KJ} - \Delta E_{\mathrm{SAC}}^{\mathrm{HF}} \bar{\bar{S}}_{KI}\right) + \frac{1}{2}\left[Q_{0I} + \sum_K Z_K \left(\bar{\bar{Q}}_{KI} - Q_{0I} \sum_J C_J \bar{S}_{KJ} - \bar{\bar{S}}_{KI}\Theta_{\mathrm{SAC}}\right)\right] \times \left[\mathrm{s}_{\mathrm{SAC}} + \sum_K Z_K \left(\sum_J C_J \bar{V}_{KJ} + V_{K0} - \mathrm{s}_{\mathrm{SAC}} \sum_J C_J \bar{S}_{KJ}\right)\right] + \frac{1}{2}\left[V_{0I} + \sum_K Z_K \left(\bar{\bar{V}}_{KI} - V_{0I} \sum_J C_J \bar{S}_{KJ} - \bar{\bar{S}}_{KI}\mathrm{s}_{\mathrm{SAC}}\right)\right] \times \left[\Theta_{\mathrm{SAC}} + \sum_K Z_K \left(\sum_J C_J \bar{Q}_{KJ} + Q_{K0} - \Theta_{\mathrm{SAC}} \sum_J C_J \bar{S}_{KJ}\right)\right]. \tag{A11}$$

Arranging Eq. (A11) as Eq. (A4), we may now write the following:

$$\frac{\partial L_{\mathrm{PCM}}^{\mathrm{SAC}}}{\partial C_I} = \bar{\bar{H}}_{0I}^{\mathrm{HF}} + \frac{1}{2}Q_{0I}\varsigma_{\mathrm{SAC}} + \frac{1}{2}V_{0I}\Theta_{\mathrm{SAC}} + \sum_K Z_K\left(\bar{\bar{H}}_{KI}^{\mathrm{HF}} - \bar{\bar{H}}_{0I}^{\mathrm{HF}}\sum_J C_J\bar{S}_{KJ} - \Delta E_{\mathrm{SAC}}^{\mathrm{HF}}\bar{\bar{S}}_{KI}\right) + \frac{1}{2}\sum_K Z_K\left(\bar{\bar{Q}}_{KI} - Q_{0I}\sum_J C_J\bar{S}_{KJ}\right.$$
$$\left. - \bar{\bar{S}}_{KI}\Theta_{\mathrm{SAC}}\right)\varsigma_{\mathrm{SAC}} + \frac{1}{2}\sum_K Z_K\left(\bar{\bar{V}}_{KI} - V_{0I}\sum_J C_J\bar{S}_{KJ} - \bar{\bar{S}}_{KI}\varsigma_{\mathrm{SAC}}\right)\Theta_{\mathrm{SAC}} + \frac{1}{2}Q_{0I}\sum_K Z_K\left(\sum_J C_J\bar{V}_{KJ} + V_{K0} - \varsigma_{\mathrm{SAC}}\sum_J C_J\bar{S}_{KJ}\right)$$
$$+ \frac{1}{2}V_{0I}\sum_K Z_K\left(\sum_J C_J\bar{Q}_{KJ} + Q_{K0} - \Theta_{\mathrm{SAC}}\sum_J C_J\bar{S}_{KJ}\right) + \frac{1}{2}\sum_K Z_K\left(\bar{\bar{Q}}_{KI} - Q_{0I}\sum_J C_J\bar{S}_{KJ} - \bar{\bar{S}}_{KI}\Theta_{\mathrm{SAC}}\right)\sum_L Z_L\left(\sum_J C_J\bar{V}_{LJ}\right.$$
$$\left. + V_{L0} - \varsigma_{\mathrm{SAC}}\sum_J C_J\bar{S}_{LJ}\right) + \frac{1}{2}\sum_K Z_K\left(\bar{\bar{V}}_{KI} - V_{0I}\sum_J C_J\bar{S}_{KJ} - \bar{\bar{S}}_{KI}\varsigma_{\mathrm{SAC}}\right)\sum_L Z_L\left(\sum_J C_J\bar{Q}_{LJ} + Q_{L0} - \Theta_{\mathrm{SAC}}\sum_J C_J\bar{S}_{LJ}\right). \quad \text{(A12)}$$

Consequently, the constant terms are

$$\bar{\bar{H}}_{0I}^{\mathrm{PCM}} = \bar{\bar{H}}_{0I}^{\mathrm{HF}} + \tfrac{1}{2}Q_{0I}\varsigma_{\mathrm{SAC}} + \tfrac{1}{2}V_{0I}\Theta_{\mathrm{SAC}}. \quad \text{(A13)}$$

The terms that are linear in Z are

$$Y_{KI}^{\mathrm{PCM}} = Y_{KI}^{\mathrm{HF}} + \frac{1}{2}\left(\bar{\bar{Q}}_{KI} - Q_{0I}\sum_J C_J\bar{S}_{KJ} - \bar{\bar{S}}_{KI}\Theta_{\mathrm{SAC}}\right)\varsigma_{\mathrm{SAC}}$$
$$+ \frac{1}{2}\left(\bar{\bar{V}}_{KI} - V_{0I}\sum_J C_J\bar{S}_{KJ} - \bar{\bar{S}}_{KI}\varsigma_{\mathrm{SAC}}\right)\Theta_{\mathrm{SAC}}$$
$$+ \frac{1}{2}Q_{0I}\left(\sum_J C_J\bar{V}_{KJ} + V_{K0} - \varsigma_{\mathrm{SAC}}\sum_J C_J\bar{S}_{KJ}\right)$$
$$+ \frac{1}{2}V_{0I}\left(\sum_J C_J\bar{Q}_{KJ} + Q_{K0} - \Theta_{\mathrm{SAC}}\sum_J C_J\bar{S}_{KJ}\right), \quad \text{(A14)}$$

where

$$Y_{KI}^{\mathrm{HF}} = \bar{\bar{H}}_{KI}^{\mathrm{HF}} - \bar{\bar{H}}_{0I}^{\mathrm{HF}}\sum_J C_J\bar{S}_{KJ} - \Delta E_{\mathrm{SAC}}^{\mathrm{HF}}\bar{\bar{S}}_{KI} \quad \text{(A15)}$$

contains the fixed HF contributions. The terms that quadratic in Z are

$$W_{KLI} = \frac{1}{2}\left(\bar{\bar{Q}}_{KI} - Q_{0I}\sum_J C_J\bar{S}_{KJ} - \bar{\bar{S}}_{KI}\Theta_{\mathrm{SAC}}\right)$$
$$\times\left(V_{L0} + \sum_J C_J\bar{V}_{LJ} - \varsigma_{\mathrm{SAC}}\sum_J C_J\bar{S}_{LJ}\right)$$
$$+ \frac{1}{2}\left(\bar{\bar{V}}_{KI} - V_{0I}\sum_J C_J\bar{S}_{KJ} - \bar{\bar{S}}_{KI}\varsigma_{\mathrm{SAC}}\right)$$
$$\times\left(Q_{L0} + \sum_J C_J\bar{Q}_{LJ} - \Theta_{\mathrm{SAC}}\sum_J C_J\bar{S}_{LJ}\right). \quad \text{(A16)}$$

Using the following vector notations for transformed matrix elements:

$$\bar{v}_K = V_{K0} + \sum_J C_J\bar{V}_{KJ}, \quad \text{(A17)}$$

$$\bar{q}_K = Q_{K0} + \sum_J C_J\bar{Q}_{KJ}, \quad \text{(A18)}$$

and

$$\bar{s}_K = S_{K0} + \sum_J C_J\bar{S}_{KJ} = \sum_J C_J\bar{S}_{KJ}, \quad \text{(A19)}$$

we obtain rather compact forms

$$Y_{KI}^{\mathrm{PCM}} = Y_{KI}^{\mathrm{HF}} + \tfrac{1}{2}\bar{\bar{Q}}_{KI}\varsigma_{\mathrm{SAC}} + \tfrac{1}{2}\bar{\bar{V}}_{KI}\Theta_{\mathrm{SAC}} - \bar{\bar{S}}_{KI}\Theta_{\mathrm{SAC}}\varsigma_{\mathrm{SAC}}$$
$$+ \tfrac{1}{2}Q_{0I}\bar{v}_K + \tfrac{1}{2}V_{0I}\bar{q}_K - \bar{s}_K(Q_{0I}\varsigma_{\mathrm{SAC}} + V_{0I}\Theta_{\mathrm{SAC}}) \quad \text{(A20)}$$

and

$$W_{KLI} = \tfrac{1}{2}\bar{\bar{Q}}_{KI}\bar{v}_L + \tfrac{1}{2}\bar{\bar{V}}_{KI}\bar{q}_L + \bar{\bar{S}}_{KI}\left(\Theta_{\mathrm{SAC}}\varsigma_{\mathrm{SAC}}\bar{s}_L - \tfrac{1}{2}\Theta_{\mathrm{SAC}}\bar{v}_L\right.$$
$$\left. - \tfrac{1}{2}\varsigma_{\mathrm{SAC}}\bar{q}_L\right) + \tfrac{1}{2}\bar{s}_K\bar{s}_L(Q_{0I}\varsigma_{\mathrm{SAC}} + V_{0I}\Theta_{\mathrm{SAC}})$$
$$- \tfrac{1}{2}\bar{s}_K(Q_{0I}\bar{v}_L + V_{0I}\bar{q}_L) - \tfrac{1}{2}\bar{s}_L(\bar{\bar{Q}}_{KI}\varsigma_{\mathrm{SAC}} + \bar{\bar{V}}_{KI}\Theta_{\mathrm{SAC}}). \quad \text{(A21)}$$

[1] W. Liptay, Angew. Chem., Int. Ed. Engl. **8**, 177 (1969); E. Buncel and S. Rajagopal, Acc. Chem. Res. **23**, 226 (1990); C. Reichardt, Chem. Rev. (Washington, D.C.) **94**, 2319 (1994).

[2] J. Kroon, J. W. Verhoeven, M. N. Paddon-Row, and A. M. Oliver, Angew. Chem., Int. Ed. **30**, 1358 (1991); P. Chen and T. J. Meyer, Chem. Rev. (Washington, D.C.) **98**, 1439 (1998); A. Vlček, Jr., Coord. Chem. Rev. **200–202**, 933 (2000); H. Imahori, M. E. El-Khouly, M. Fujitsuka, O. Ito, Y. Sakata, and S. Fukuzumi, J. Phys. Chem. A **105**, 325 (2001); F. Barrière, N. Camire, W. E. Geiger, U. T. Mueller-Westerhoff, and R. Sanders, J. Am. Chem. Soc. **124**, 7262 (2002).

[3] Y. Xu, W. K. Chen, M. J. Cao, S. H. Liu, J. Q. Li, A. I. Philippopoulos, and P. Falaras, Chem. Phys. **330**, 204 (2006); C. Barolo, M. K. Nazeeruddin, S. Fantacci, D. Di Censo, P. Comte, P. Liska, G. Viscardi, P. Quagliotto, F. De Angelis, S. Ito, and M. Grätzel, Inorg. Chem. **45**, 4642 (2006); M. K. Nazeeruddin, T. Bessho, L. Cevey, S. Ito, C. Klein, F. De Angelis, S. Fantacci, P. Comte, P. Liska, H. Imai, and M. Grätzel, J. Photochem. Photobiol., A **185**, 331 (2007).

[4] H. Nakatsuji and K. Hirao, Chem. Phys. Lett. **47**, 569 (1977); J. Chem. Phys. **68**, 2053 (1978).

[5] H. Nakatsuji, Chem. Phys. Lett. **59**, 362 (1978); **67**, 329 (1979); **67**, 334 (1979).

[6] K. Emrich, Nucl. Phys. A **351**, 379 (1981); J. Geertsen, M. Rittby, and R. J. Bartlett, Chem. Phys. Lett. **164**, 57 (1989); D. C. Comeau and R. J. Bartlett, *ibid.* **207**, 414 (1993); J. F. Stanton and R. J. Bartlett, J. Chem. Phys. **98**, 7029 (1993).

[7] H. Monkhorst, Int. J. Quantum Chem., Quantum Chem. Symp. **11**, 421

(1977); E. Dalgaard and H. Monkhorst, Phys. Rev. A **28**, 1217 (1983); D. Mukherjee and P. K. Mukherjee, Chem. Phys. **39**, 325 (1979); M. Takahashi and J. Paldus, J. Chem. Phys. **85**, 1486 (1986).
[8] H. Koch and P. Jørgensen, J. Chem. Phys. **93**, 3333 (1990); H. Koch and H. J. Aa. Jensen, P. Jørgensen, and T. Helgaker, *ibid.* **93**, 3345 (1990).
[9] H. Nakatsuji, Bull. Chem. Soc. Jpn. **78**, 1705 (2005); J. Hasegawa and H. Nakatsuji, in *Radiation Induced Molecular Phenomena in Nucleic Acid: A Comprehensive Theoretical and Experimental Analysis*, edited by M. Shukla and J. Leszczynsk (Springer, New York, 2008), Chapts. 4 and 93–124; M. Ehara, J. Hasegawa, and H. Nakatsuji, in *Theory and Applications of Computational Chemistry: The First 40 Years, A Volume of Technical and Historical Perspectives*, edited by C. E. Dykstra, G. Frenking, K. S. Kim, and G. E. Scuseria (Elsevier, Oxford, 2005), pp. 1099–1141.
[10] S. Miertuš, E. Scrocco, and J. Tomasi, Chem. Phys. **55**, 117 (1981).
[11] J. Tomasi, B. Mennucci, and R. Cammi, Chem. Rev. (Washington, D.C.) **105**, 2999 (2005).
[12] J. S. Arponen, R. F. Bishop, and E. Pajanne, Phys. Rev. A **36**, 2519 (1987).
[13] E. A. Salter, G. W. Trucks, and R. J. Bartlett, J. Chem. Phys. **90**, 1752 (1989); R. J. Bartlett, in *Modern Electronic Structure Theory, Part II*, edited by D. R. Yarkony (World Scientific, Singapore, 1995), pp. 1047–1131.
[14] H. Koch and H. J. Aa Jensen, P. Jørgensen, T. Helgaker, G. E. Scuseria, and H. F. Schaefer III, J. Chem. Phys. **92**, 4924 (1990).
[15] O. Christiansen and K. V. Mikkelsen, J. Chem. Phys. **110**, 1365 (1999); **110**, 8348 (1999); A. Osted, J. Kongsted, K. V. Mikkelsen, and O. Christiansen, Mol. Phys. **101**, 2055 (2003).
[16] T. Nakajima and H. Nakatsuji, Chem. Phys. **242**, 177 (1999).
[17] R. Cammi, J. Chem. Phys. **131**, 164104 (2009).
[18] F. J. Olivares del Valle and J. Tomasi, Chem. Phys. **150**, 134 (1991); M. Aguilar, F. J. Olivares del Valle, and J. Tomasi, *ibid.* **150**, 151 (1991); F. J. Olivares del Valle, R. Bonacorsi, R. Cammi, and J. Tomasi, J. Mol. Struct.: THEOCHEM **230**, 295 (1991); F. J. Olivares del Valle, M. Aguilar, and S. Tolosa, *ibid.* **279**, 223 (1993); F. J. Olivares del Valle and M. Aguilar, *ibid.* **280**, 25 (1993).
[19] J. Hasegawa, S. Bureakaw, and H. Nakatsuji, J. Photochem. Photobiol., A **189**, 205 (2007).
[20] J. F. Stanton, J. Chem. Phys. **99**, 8840 (1993); J. F. Stanton and J. Gauss, *ibid.* **100**, 4695 (1994); **101**, 8938 (1994).
[21] R. Cammi, S. Corni, B. Mennucci, and J. Tomasi, J. Chem. Phys. **122**, 104513 (2005).
[22] J. Frenkel, *Wave Mechanics-Advanced General Theory* (Oxford University Press, Oxford, 1979); R. Cammi and J. Tomasi, Int. J. Quantum Chem. **60**, 297 (1996).
[23] J. Olsen and P. Jørgensen, in *Modern Electronic Structure Theory, Part II*, edited by D. R. Yarkony (World Scientific, Singapore, 1995).
[24] S. Corni, R. Cammi, B. Mennucci, and J. Tomasi, J. Chem. Phys. **123**, 134512 (2005).
[25] M. Caricato, B. Mennucci, J. Tomasi, F. Ingrosso, R. Cammi, S. Corni, and G. Scalmani, J. Chem. Phys. **124**, 124520 (2006).
[26] J. Kongsted, A. Osted, K. V. Mikkelsen, and O. Christiansen, Mol. Phys. **100**, 1813 (2002).
[27] B. Mennucci, R. Cammi, and J. Tomasi, J. Chem. Phys. **109**, 2798 (1998).
[28] R. A. Marcus, J. Chem. Phys. **24**, 966 (1956).
[29] A. Klamt, J. Phys. Chem. **100**, 3349 (1996).
[30] R. Cammi and J. Tomasi, Int. J. Quantum Chem. Symp. **56**, 465 (1995); M. A. Aguilar, J. Phys. Chem. A **105**, 10393 (2001).
[31] H. M. Senn and W. Thiel, Angew. Chem., Int. Ed. **48**, 1198 (2009).
[32] J. Gao and X. Xia, Science **258**, 631 (1992); J. Gao, J. Am. Chem. Soc. **115**, 2930 (1993); M. L. Sánchez, M. E. Martín, M. A. Aguilar, and F. J. Olivares del Valle, Chem. Phys. Lett. **310**, 195 (1999).
[33] J. Gao, J. Comput. Chem. **18**, 1061 (1997); J. Kongsted, A. Osted, K. V. Mikkelsen, and O. Christiansen, J. Chem. Phys. **118**, 1620 (2003).
[34] M. Caricato, B. Mennucci, G. Scalmani, G. W. Trucks, and M. J. Frisch, J. Chem. Phys. **132**, 084102 (2010).
[35] R. Fukuda and H, Nakatsuji, J. Chem. Phys. **128**, 094105 (2008).
[36] G. Mackinney and O. Temmer, J. Am. Chem. Soc. **70**, 3586 (1948).
[37] K. Inuzuka, Bull. Chem. Soc. Jpn. **33**, 678 (1960).
[38] A. F. Moskvin, O. P. Yablonskii, and L. F. Bondar, Theor. Exp. Chem. **2**, 636 (1966).
[39] A. M. D. Lee, J. D. Coe, S. Ullrich, M.-L. Ho, S.-J. Lee, B.-M. Cheng, M. Z. Zgierski, I-C. Chen, T. J. Martínez, and Albert Stolow, J. Phys. Chem. A **111**, 11948 (2007).
[40] S. Iwata and K. Morokuma, J. Am. Chem. Soc. **97**, 966 (1975); S. Tenno, F. Hirata, and S. Kato, J. Chem. Phys. **100**, 7443 (1994); H. C. Georg, K. Coutinho, and S. Canuto, *ibid.* **123**, 124307 (2005); G. Brancato, N. Rega, and V. Barone, *ibid.* **125**, 164515 (2006); S. A. do Monte, T. Müller, M. Dallos, H. Lischka, M. Diedenhofen, and A. Klamt, Theor. Chem. Acc. **111**, 78 (2004).
[41] F. Aquilante, V. Barone, and B. O. Roos, J. Chem. Phys. **119**, 12323 (2003).
[42] M. E. Martín, A. Muñoz Losa, and I. Fdez -Galván, and M. A. Aguilar, J. Chem. Phys. **121**, 3710 (2004).
[43] A. Muñoz Losa and I. Fdez Galván, M. A. Aguilar, and M. E. Martín, J. Phys. Chem. B **111**, 9864 (2007).
[44] K. Aidas, A. Møgelhøj, E. J. K. Nilsson, M. S. Johnson, K. V. Mikkelsen, O. Christiansen, P. Söderhjelm, and J. Kongsted, J. Chem. Phys. **128**, 194503 (2008).
[45] B. Saha, M. Ehara, and H. Nakatsuji, J. Chem. Phys. **125**, 014316 (2006).
[46] R. P. Johnson and M. W. Schmidt, J. Am. Chem. Soc. **103**, 3244 (1981).
[47] S. W. Staley and T. D. Norden, J. Am. Chem. Soc. **106**, 3699 (1984).
[48] R. Cammi, L. Frediani, B. Mennucci, J. Tomasi, K. Ruud, and K. V. Mikkelsen, J. Chem. Phys. **117**, 13 (2002).
[49] M. Merchán, R. González-Luque, and B. O. Roos, Theor. Chim. Acta **94**, 143 (1996).
[50] M. J. Frisch, G. W. Trucks, H. B. Schlegel *et al.*, GAUSSIAN, Revision H.06, Gaussian Inc., Wallingford, CT, 2009.
[51] R. J. Bartlett and M. Musiał, Rev. Mod. Phys. **79**, 291 (2007).
[52] T. Nakajima and H. Nakatsuji, Chem. Phys. Lett. **280**, 79 (1997).
[53] A. Dalgarno and A. L. Stewart, Proc. R. Soc. London, Ser. A **247**, 245 (1958); N. C. Handy and H. F. Schaefer III, J. Chem. Phys. **81**, 5031 (1984).
[54] R. Cammi, L. Frediani, B. Mennucci, and K. Ruud, J. Chem. Phys. **119**, 5818 (2003).
[55] H. Nakatsuji, M. Hada, M. Ehara, K. Toyota, R. Fukuda, J. Hasegawa, M. Ishida, T. Nakajima, Y. Honda, O. Kitao, and H. Nakai, SAC-CI guide, 2005, PDF file is available at http://www.qcri.or.jp/sacci/.
[56] R. Cammi and J. Tomasi, J. Chem. Phys. **100**, 7495 (1994).
[57] K. Toyota, M. Ishida, M. Ehara, M. J. Frisch, and H. Nakatsuji, Chem. Phys. Lett. **367**, 730 (2003).
[58] R. Cammi, B. Mennucci, and J. Tomasi, J. Phys. Chem. A **103**, 9100 (1999).
[59] T. H. Dunning, Jr., J. Chem. Phys. **90**, 1007 (1989).
[60] H. Nakatsuji, Chem. Phys. **75**, 425 (1983); H. Nakatsuji, J. Hasegawa, and M. Hada, J. Chem. Phys. **104**, 2321 (1996).
[61] E. Cancès and B. Mennucci, J. Math. Chem. **23**, 309 (1998); E. Cancès, B. Mennucci, and J. Tomasi, J. Chem. Phys. **107**, 3032 (1997); B. Mennucci, E. Cancès, and J. Tomasi, J. Phys. Chem. B **101**, 10506 (1997).
[62] M. J. Frisch, G. W. Trucks, H. B. Schlegel *et al.*, GAUSSIAN 09, Revision A.02, Gaussian Inc., Wallingford, CT, 2009.
[63] E. A. Cherniak and C. C. Costain, J. Chem. Phys. **45**, 104 (1966).
[64] C. E. Blom, G. Grassi, and A. Bauder, J. Am. Chem. Soc. **106**, 7427 (1984).
[65] J. M. Hollas, Spectrochim. Acta, Part A **19**, 1425 (1963).
[66] M. Reguero, M. Olivucci, F. Bernardi, and M. A. Robb, J. Am. Chem. Soc. **116**, 2103 (1994); W.-H. Fang, *ibid.* **121**, 8376 (1999); A. Muñoz Losa, M. E. Martín, and I. Fdez. Galván, and M. A. Aguilar, Chem. Phys. Lett. **443**, 76 (2007).
[67] R. S. Becker, K. Inuzuka, and J. King, J. Chem. Phys. **52**, 5164 (1970).
[68] A. D. Walsh, Trans. Faraday Soc. **41**, 498 (1945).
[69] T. D. Norden, S. W. Staley, W. H. Taylor, and M. D. Harmony, J. Am. Chem. Soc. **108**, 7912 (1986).
[70] K. Sneskov, E. Matito, J. Kongsted, and O. Christiansen, J. Chem. Theory Comput. **6**, 839 (2010).